

Response to Reviewer Number 3:

We thank reviewer number 3 for his/her comments. In particular, we will focus on the data quality issues here. We also will focus on the expansion of the overall amount of data used, so as to reinforce the validity and uniqueness of this approach. We greatly appreciate all of the depth and complexity, and hope that our hard work has addressed the various suggestions improvements recommended.

The Reviewer's comments in italics, while our specific responses are in plain text.

"1. The plume height analysis entirely depends on CALIPSO extinction profiles and vertical feature mask product. However, both these two products bare uncertainties that could contaminate the results. Especially that the feature classification is based on lidar ratio which is highly uncertain. The author should provide evidence that these data are validated against ground based lidar for the region and period of interest."

We have carefully analyzed the MPL data from the Singapore station, which exists within the "Fire-Region" in this study. We find that throughout the period, the general average mean extinction height varies from 1.8km through 2.1km, which is consistent with the statistical results found using CALIPSO. Hence, we believe we have done at least as well as others, with respect to validating the variables used, over this region. We have added in Supplemental Figure 3 and the following text:

"These results are supported by the statistical values of aerosol heights measured by the MPL station in Singapore throughout the period from September 1 to November 30 (**Supplemental Figure 3**), which are found to range from 1.6km to 2.4km. While there were no ground-based lidar measurements available in 2006, the year 2015 was another very strong El-Nino year which impacted Singapore with severe downwind aerosols from burning sources, and closely resembled 2006."

"2. The fire region is selected according to MISR AOD. While I agree that MISR cloud screen might be better than MODIS, its sampling is rather poor over low latitudes. This means that many small scale plumes may not be captured by MISR at all. I suggest the authors compare both MODIS and MISR and maybe also OMI which is good in measuring absorbing aerosols to better determine the fire region or to confirm their defined region."

Due to the extensive spatial distribution of the fires, there are almost no visible plumes over this region. They all intermix, and effectively act as a single plume. This is clearly mentioned in the text. In previous work already cited here, we have found that MISR performs better than MODIS in this region of the world, when compared against AERONET. However, we have also used MODIS in this study, as demonstrated in **Figure 2** and **Supplemental Figure 2**. To validate our assertion, we have found that the actual spatial area of cloud-free measurements provided by MODIS is considerably less than MISR. However, the fact that a similar conclusion is made, that the "Fire-Region" has a much higher AOD than the "Non-Fire-Region", means that these different platforms are at least achieving a similar large-scale result.

47
48 “3. The authors state that the CALIPSO statistics is based on more than 10,000 profiles.
49 In my opinion, it is not the number of profiles that matters but the number of plumes or
50 fire events that the sampling represents. Usually one plume or event may contain tens or
51 even hundreds of profiles. So are these 10,000 profiles complete or representative or the
52 entire biomass burning season?”

53
54 The CALOIP passes are as representative of the total fires as is possible. Every single
55 measurement that intersects the geographical region of interest, is used. Additionally, due
56 to the frequency of the passes, there is enough sampling done to account for any localized
57 events in space or time that may not be representative of the overall fire statistics. To
58 address the issue of representativeness in time, we have expanded the paper’s analysis to
59 encompass the entire fire season the paper, now using three months of measurements,
60 from September 1st to November 30th. The fire season was found to extend from
61 September 3rd through November 9th. And within this period as a whole, the findings are
62 similar, with the results not significantly changing. Please see the updated results in
63 **Figure 2, Figure 3a, and Table 1.**

64 In fact, the only observed change is that the measured heights are slightly lower when
65 also incorporating in the data from September 3rd to September 30th and from November
66 1st to November 9th. This is consistent with the fact that while both September and
67 November recorded as significant in the past work, that the difference in the measured
68 AOD between the fire-region and non-fire region during this time was smaller than
69 during the October peak. Again, this reinforces the robustness and inclusivity of this
70 approach.

71 The first conclusion, as already mentioned in this work and previous work, it is
72 impossible to talk about “number of plumes” or “number of fire events”. The entire
73 region is burning, or such a significant amount of the region, that in effect, there is just a
74 single giant plume as far as the atmosphere is concerned. The entire idea of counting
75 individual plumes is outdated, and not really possible. In the atmosphere, due to the
76 amount of fires, and their density, the overall distribution behaves as a “single massive
77 plume”.

78
79 “4. The conclusion that fire power is underestimated is solely based on matching the
80 plume rise model with CALIPSO observed mid plume height. However, the model still
81 shows quite different low and high plume heights. Given that the latter two is also related
82 to emission power, the conclusion seems unsound.”

83
84 We believe that the best fit matches with the data for other plume heights are also
85 mentioned in the text. In fact, we specifically stated that a nearly doubling of the radiative
86 power is required to match with the middle-upper height. We additionally talk about how
87 there are other, higher-order and non-linear feedbacks, that impact the system, that are
88 beyond the scope of this analysis, but are consistent with the findings here, especially for
89 the top and bottom values. The basic point is that even a scaled plume-rise approach will
90 not be able to accurately reproduce the top or bottom of the plume, under the conditions
91 observed in this environment.

This is especially so in the cloudy tropics. Under such intense radiation, strongly absorbing smoke aerosol has significant impacts on the direct effect (near the bottom of the column) and the semi-direct effect (near the top of the column). Furthermore, local convection may also impact the plume rise height. This is already mentioned in the paper.

“5. I still have some problem with the claim that the result of the current paper is very different from previous studies. This is also the main issue raised by the first round of reviewers. The authors cited Tosca et al. (2011) who stated that the plumes are mostly confined within the boundary layer. The Tosca et al. results are based on the entire 2001-2009 period rather than just October 2006, therefore not directly comparable with the current study. The authors need to be more careful about their statement and conclusion and provide direct comparisons with previous research.”

First of all, the majority of fires occurring during the period from September through November, occur in this region of the world. Secondly, 2006 was specifically chosen, as it was one of the years with the most available amounts of smoke events, due to the dryness associated with El-Nino. This was also clearly mentioned in Tosca et al. (2011). In fact, their paper also specifically pointed to October 2006 as a case study, and hence a direct comparison is indeed able to be made. This is why we have extended our analysis from September 1st to November 30th, so that we can capture the entire breadth of the fire season. In addition, other such papers have also now been cited in the latest update, including: Campbell, et al. (2013); Lee, et al. (2016); Sugimoto, et al. (2014a); and Sugimoto, et al. (2014b). It is true that there are not many papers with respect to this region, and furthermore it is true that none of the available other works have gone into the depth and clarity with how they have analyzed the data, and hence, it may not be possible to find any more closely-related work.

“6. Lines 162-163: is the resolution 10km or 1km? Also I suggest the authors change the “x” in “10kmx10km” to the real multiplication signs by inserting symbols.”

The symbol issue has been taken care of. Thank you for pointing this out. The resolution is 10km for the AOD product and 1km for the FRP and fire temperature products.

“7. Lines 183-185: please provide references that AOD and other products are validated.”

Additional references indicating AOD validation have been included.

“8. Lines 258-260: I don’t understand this sentence. Please rephrase.”

This has been re-written. Thank you.

“9. Line 289: “this work’s underlying Kalman Filter plus variance maximization inversely modeled fields”, is this used in the plume rise model? If so, please describe more specifically in the model description section.”

This is the spatial region that is used for defining the “Fire-Region” and the “non-Fire-Region”. This is now made more clear in the text.

“10. Line 325: lower temperature should correspond to “lower emission factor” rather than “higher aerosol emission factor”.”

We think it is much more complex than this, and hence disagree to making this change. Lower temperature should correspond to a lesser amount of burnt material, and hence a lower absolute emissions of total carbon to the atmosphere. However, sometimes at lower temperatures, especially in the wet tropics, the actual mass of aerosol being produced is higher. This has to do with the water content leading to less oxygen being available for combustion, and the combustion occurring at a lower temperature. In the end, this leads to more incomplete combustion, and hence more volatile species being produced, as well as BC and OC emissions. Frequently at very high temperature, these species are more highly oxidized and hence have less mass remaining in the aerosol phase. Thank you for this interesting point, as it provides a future basis upon which to continue looking more deeply into the topics raised here.

“11. Line 400-401: This statement is too strong. Given the data quality problem and model mismatch problem, I don’t think the work “comprehensively quantifies ... ”.”

The suggestion has been addressed and the sentence re-worded.

“12. The paper still has many grammar mistakes, such as verbs associated with plural or single forms. Please double check”

Thank you for pointing this out. A careful review has found some additional errors and fixed them.

Response to Reviewer Number 4:

“The manuscript uses satellite-derived AOD to spatially and temporally constrain the sampling of smoke aerosols with an aim to examine the aerosol vertical distributions, measured from CALIOP, over the maritime continent during the 2006 El Nino. The observed aerosol vertical distributions were then used to compare with the results of a simple plume rise model. The study provides some insights into the aerosol signature in terms of vertical distribution during El Nino conditions and the limitations of plume rise models. But additional evidences and analysis are required to support the conclusions. Several major comments have to be addressed. Furthermore, the manuscript readability and clarity has to be improved before the publication in ACP.”

Thank you very much for your deeply reflective and insightful comments. We have carefully parsed through them and worked our hardest to address them. We have done significantly more work and analytics, as well as extending the period of the data analyzed. Overall our same conclusions are found, but they are now strengthened. By extending the analysis to the entire fire season, not just the peak of the fire season, we have more conclusively exhibited our findings, and determined that the underlying points are still the same. We still find that the vast majority of the measured aerosol is in the free troposphere. Second, that the existing plume models are biased in terms of reproducing the lower portions of the plume, and are not capable of reproducing the extremes in the plume height. Third, that the underestimation of measured FRP leads to an improvement in being able to model the central characteristics of the plume, even given the uncertainty in average boundary layer characteristics, if FRP enhancements are applied piecemeal. However, fourth, that to model some essential statistics, such as the plume distribution, or the extreme plume height values, that fundamental changes to the models themselves will need to be made. We have also spent extensive time and care to re-write the paper and make it more readable.

“1. More elaborations and descriptions are required for CALIPSO data processing. Which version and level of CALIOP product? Is each individual measurement under cloud-free conditions? If yes, which cloud mask data was used? How many samples in total? What is the threshold value of extinction from CALIOP data (please consider the daytime background solar illumination by Winker et al., 2013)? In addition, an analysis of the uncertainties of the CALIOP-derived vertical aerosol extinction, in particular over this region, is needed.”

Thank you very much for your detailed suggestions. A couple of paragraphs and sentences have been added addressing the data processing, cloud-conditions, masking data, and number of samples in total. In addition, we have thoroughly read your paper cited it, and included some specific points from it, since we believe that it strengthens the overall conclusion.

We do agree with you that a deeper study of aerosol extinction over this region is warranted, and possibly can follow-up in a future, more detailed analysis. However, at the present time, we do not consider or use the extinction data from CALIOP in this work, only from MODIS and MISR.

213
214 “2. The effects of the uncertainty in boundary layer depth need to be considered. The
215 authors simply use the 1000 m to approximate the boundary layer height. Assuming the
216 boundary layer has +/- 300 m uncertainties during the CALIPSO overpass, which is
217 totally possible, what are the uncertainties of the percentage of free atmosphere aerosol
218 estimated by your method? When taking this into account, how does your result compare
219 with previous studies?”
220

221 This is a very fair comment, especially given the uncertainty in boundary layer height in
222 the tropics. The analysis has been expanded to include this uncertainty band, and the
223 results have been correspondingly updated throughout the manuscript. The findings show
224 that the elevated levels during the October maximum are more significant than the entire
225 fire season, but that this difference is considerably smaller than between the fire-region
226 and the non fire-region. Furthermore, the difference between the boundary layer
227 uncertainty is also considerably smaller than between the fire-region and the non fire-
228 region. Hence, the results have been statistically strengthened by this analysis.
229 **Therefore, many thanks again for this suggestion**, even though it took a considerable
230 amount of time to properly implement.
231

232 “3. The author uses aerosol-induced in-situ stabilization as a possible explanation to the
233 underestimation of plume height by model. But the rationale seems problematic. The
234 model does not account for the effect of aerosol-induced stabilization which actually
235 happens in the real atmosphere. The stabilization causes weaker buoyancy, thus lower
236 plume height. Therefore the model that misses such stabilization should overestimate, not
237 underestimate, the plume height.”
238

239 Actually, this is a very important point and it has been re-explained further in the text. We
240 agree with you that, at the surface, the aerosol effect reduces the buoyancy, by reducing
241 the incoming solar radiation. However, due to the large amount of highly absorbing
242 aerosols, it actually increases buoyancy near the top of the plume. And this increase is
243 further enhanced by the fact that once the aerosols are over the cloud top (as observed),
244 that this absorption is doubled. Hence, it serves the effect of reducing the heights near the
245 bottom, while simultaneously increasing the heights near the top. On the other hand, if
246 the surface fire radiative power were higher, say to the extent that most of the plume were
247 lofted to or above the cloud deck, which is what is observed, then this would not be the
248 case. The reduced buoyancy due to the aerosol direct effect is overcome near the bottom
249 by the additional heating. While on the other hand, the spread at the top would be
250 increased, due to the additional heating. Hence, a bias would occur, where the top of the
251 plume would be found to be biased slightly higher, which is what the measurements
252 seemingly demonstrate.
253

254 “4. The comparison between model and observation is insufficient. The observation
255 misses 3 days and the model misses 9 days with only 18 days left. This is rather a small
256 sample. Since the fires lasts from September to November, it is worthwhile to expand the
257 analysis to September and November. In addition, the analysis is primarily limited to the
258 monthly averages. The authors do show the comparisons in daily basis in Figure 4, but

do not analyze them. In particular, the three special days mentioned in section 3.2 are good example cases to analyze in order to shed more light on the observation-model comparisons. Such more comprehensive analysis is very worthwhile in order to support the conclusions of how to reduce model bias which is actually not well examined or indicated in the manuscript."

The analysis has been increased to the entire time period corresponding with the increase in measurements and still constrained by the MODIS observations of being within the fire season. There are now a total of 47 days in common to be analyzed. As is expected, including the additional days has led to the mismatch between the model and the measurements to be less large, but it has not changed the statistical significance, the sign, or the overall value significantly. Details have been addressed in an updated **Figure 4** and in the text. This includes some details of special days as well. As expected, the maximum and most intense part of the fire season, October, has the largest mis-match. However, the bias in the model mismatch, in particular for the median and lower plume heights, and the large majority of the plume still being measured in the lower free troposphere are still consistent across the entire fire season. Just less so over the entire fire season. This additional work has strongly enhanced the overall results of the work.

"Line 15: "measurements and modeling". Please specify which measurement and which model."

This has been modified and explained in more detail.

"Line 16: "underestimated" by what?"

This has been addressed.

"Line 51: Sentence not readable"

This has been addressed.

"Line 53 ~ 54: "underestimation" in "spatial, and temporal distribution"? "

This has been made clear.

"Line 60: Change "show" to "shown" "

Done.

"Line 75: Show full name of "CALIOP" "

Inserted at the first point CALIOP is mentioned.

"Line 77: Show full name of "SSA" "

305 Inserted at the first point SSA is mentioned.
306
307 *“Line 77: “go with each pass”. Is it scientific language? ”*
308
309 This has been updated to be more technical and precise.
310
311 *“Line 82: grammar error”*
312
313 This has been rewritten.
314
315 *“Line 85: Show full name of “MISR” ”*
316
317 Done.
318
319 *“Line 157: Please provide the reference. ”*
320
321 Done.
322
323 *“Line 158: delete one “are” ”*
324
325 Done
326
327 *“Line 162~167: Show full name of “AERONET”, “NOAA”, “RMS”, “RCP”, “GDED” ”*
328
329 Done
330
331 *“Line 167: what is R2 statistic? ”*
332
333 Coefficient of determination. It relates the amount of variance observed in the response
334 variable by the test variable. This commonly used statistic has been defined more clearly
335 and in more depth.
336
337 *“Line 204~206: Please provide new plot to show them more directly. ”*
338
339 **Figure 4** has been both updated to demonstrate the additional days of model results, as
340 well as being completely reformatted to make it clearer and easier to understand and
341 interpret. Thank you for the suggestion.
342
343 *“Line 218: Show full name of “BC” ”*
344
345 Done.
346
347 *“Line 272: add “of” after “and” ”*
348
349 Done.
350

351 *“Line 285~286: Why not examining the hypothesis by looking at precipitation data from*
352 *ATrain? ”*

353
354 This has now been done in depth. One and a half paragraphs have been added to the
355 manuscript, as well as a Supplemental figure. The results support the previous hypothesis.

356
357 “One consistent rationale is that there was large-scale precipitation event at that time,
358 which in turn both increased aerosol removal and wetting of the surface. This in turn led
359 to lower temperature and FRP and correspondingly higher aerosol emissions factor on
360 these days. Overall, there is no apparent impact of day-to-day variability of measured
361 FRP driving observed variation in measured aerosol heights, and hence only high
362 confidence fire data is subsequently used.

363 To examine this hypothesis, the GPCP [Global Precipitation Climatology Project]
364 One-Degree Daily Precipitation Data Set of global precipitation has been employed to
365 study the amount and duration of rainfall over the fire-burning and non fire-burning
366 regions [Huffman et al., 2012]. A spatial/temporal analysis of this dataset, over both the
367 Fire Region and the No-Fire region confirms this hypothesis (**Supplemental Figure 4**)
368 Supp. Overall, there was considerably lower rainfall over the Fire Region than the No-
369 Fire Region, however, on all days that there was a decrease in AOD and FRP over the
370 Fire Region, there was a heavy Rainfall at the same time, or one or two days before. The
371 measurements have a correlation coefficient of -0.39 with a corresponding $p < 0.01$. There
372 is no other statistically significant correlation found over any other combination of the
373 regions with any other combination of rainfall.”

374
375 *“Line 290: Show full name of “MERRA” ”*

376
377 Done. The sentence has also been re-written.

378
379 *“Line 360-361: “vertical distribution” is not a parameter to be “estimated”. ”*

380
381 This has been addressed.

382
383 *“Figure 1: What does the color stand for? Please add a title to the colorbar. ”*

384
385 This has been added to the figure caption.

386
387 *“Figure 4: The comparison is really not readable. Please make it more clear. ”*

388
389 This has been addressed in the new **Figure 4**.

Vertical distribution of aerosols over the Maritime Continent during El Nino

Jason Blake Cohen¹, Daniel Hui Loong Ng², Alan Wei Lun Lim³, Xin Rong Chua⁴

¹School of Atmospheric Sciences, Sun Yat-Sen University, Guangzhou, China

²Tropical Marine Science Institute, National University of Singapore, Singapore

³The Chinese University of Hong Kong, Hong Kong, China

⁴Princeton University, Princeton, NJ, USA

Correspondence to: Jason Blake Cohen (jasonbc@alum.mit.edu)

Abstract. The vertical distribution of aerosols over Southeast Asia, a critical factor impacting aerosol lifetime, radiative forcing, and precipitation, is examined for the 2006 post El-Nino fire burning season. Combining these measurements with remotely sensed land, fire, and meteorological measurements, and fire plume modeling, we have reconfirmed that fire radiative power is underestimated over Southeast Asia by MODIS measurements. These results are derived using a significantly different approach. The horizontally constrained Maritime Continent's fire plume median height, using the maximum variance of satellite observed Aerosol Optical Depth as the spatial and temporal constraint, is found to be 2.04 ± 1.52 km during the entirety of the 2006 El Nino fire-season, and 2.19 ± 1.50 km for October 2006. This is 0.83 km (0.98 km) higher than random sampling and all other past studies. Additionally, it is determined that $61(+6-10)\%$ of the bottom of the smoke plume and $83(+8-11)\%$ of the median of the smoke plume is in the free troposphere during the October maximum; while correspondingly $49(+7-9)\%$ and $75(+12-12)\%$ of the total aerosol plume and the median of the aerosol plume, are found in the free troposphere during the entire fire-season. The vastly different vertical distribution will have impacts on aerosol lifetime and dispersal. Application of a simple plume rise model using measurements of fire properties underestimates the median plume height by 0.26 km over the entire fire season and 0.34 km over the Maximum fire period. It is noted that the model underestimation over the bottom portions of the plume are much larger. The center of the plume can be reproduced when fire radiative power is increased by 20% (with other parts of the plume ranging from an increase of 0% to 60% depending on the portion of the plume and the length of the fire season considered). However, to reduce the biases found, improvements including fire properties under cloudy conditions, representation of small scale convection, and inclusion of aerosol direct and semi-direct effects is required.

- Deleted: of
- Deleted: , and impact on
- Deleted: Additionally, through
- Deleted: analysis of
- Deleted: measurements
- Deleted: the hypothesis
- Deleted: Our results are
- Deleted:
- Deleted: from what others are using
- Deleted: 17
- Deleted: 3
- Deleted: during the entirety of the 2006 El Nino fire-season, and 2.1720 ± 1.530 km for October 2006
- Deleted: 96
- Deleted: (0.99 km)
- Deleted: ,
- Deleted: with
- Deleted: 62%
- Formatted: Not Highlight
- Formatted: Not Highlight
- Deleted: particles
- Formatted: Not Highlight
- Deleted: in the free troposphere
- Deleted: is that the
- Deleted: will be considerably longer, and that the aerosols will
- Deleted: e in a direction different from if they were in the boundary layer
- Deleted: and more in the bottom-half of the plume
- Deleted:
- Deleted: e
- Deleted: 100%
- Deleted: are required in terms of measurements of f
- Deleted: when cloud covered
- Deleted: representation of
- Deleted: The results provide the unique aerosol signature of fire under El-Nino conditions.

1. Introduction

Properly quantifying the vertical distribution of aerosols is essential to constrain their atmospheric distribution, and in turn, the atmospheric energy budget [Ming *et al.*, 2010; Kim *et al.*, 2008], and understand their impact on circulation, clouds and precipitation [Tao *et al.*, 2012; Wang 2013], and human health [Burnett *et al.*, 2014]. However, there are complicating factors including spatial and temporal heterogeneity in emissions [Cohen and Wang, 2014; Cohen, 2014; Giglio *et al.*, 2006; Petrenko *et al.*, 2012; Wooster *et al.*, 2012], and uncertainties and non-linearities associated with aerosol processing and removal from the atmosphere [Tao *et al.*, 2012; Cohen and Prinn, 2011; Cohen *et al.*, 2011]. Furthermore, a lack of sufficiently dense measurements leads to difficulty constraining the measured distribution of aerosols over scales from hundreds to thousands of kilometers or over time frames on the decadal to longer time scales [Cohen and Wang, 2014; Delene and Ogren, 2002; Dubovik *et al.*, 2000; Cohen *et al.*, 2017].

Models are very poor at reproducing the actual vertical distribution of atmospheric aerosols [Cheng *et al.*, 2012; Schuster *et al.*, 2005; Tsigaridis *et al.*, 2014]. They also tend to strongly underestimate the total atmospheric column loading of aerosols [Colarco *et al.*, 2004; Leung *et al.*, 2007]. Furthermore, vertical measurements are sparse, and in many regions do not provide adequate statistics to make informed comparisons with real world conditions. This is no more apparent than over Southeast Asia, where model studies [Tosca *et al.*, 2011; Martin *et al.*, 2012] have concluded that almost all aerosols are narrowly confined in the planetary boundary layer, although measurements demonstrate otherwise [Lin *et al.*, 2014]. Presently, there are no known modeling efforts that have been able to reproduce this significant atmospheric loading and the ensuing vertical distribution.

Additionally, aerosol emissions databases in Southeast Asia are quantified using a bottom-up approach, where small samples and statistics of the activity, land-use, economics, population, and hotspots are aggregated [van der Werf, 2010; Lamarque, 2010; Bond *et al.*, 2004]. This problem is further exacerbated by the fact that emissions from organic soils are already not well studied even in non-tropical regions (Urbanski, 2014). This generally leads to sizable bias, since there are few measurements and rapidly changing land-surface features over Southeast Asia. A recent couple of papers, using measurements and models in tandem, has quantified a significant underestimation in aerosol emissions over Southeast Asia in terms of magnitude [Cohen and Wang, 2014], as well as in terms of the spatial and temporal distribution of the emissions [Cohen, 2014], including interannual and intraannual variation from fires.

Furthermore, the vertical distribution is uncertain due to incomplete understanding of in-situ production and removal mechanisms, which are dependent on washout, which is also poorly modeled [Tao *et al.*, 2012; Wang 2013], especially in the tropics during the dry season [Petersen and Rutledge, 2001; Ekman *et al.*, 2012], due to the random nature of convective precipitation. Heterogeneous aerosol processing may also change the hygroscopicity and hence vertical distribution of the aerosols [Kim *et al.*, 2008; Cohen *et al.*, 2011]. These factors have been shown to combine such that small changes in the initial vertical distribution can lead to ultimate transport thousands of kilometers apart [Wang, 2013].

Deleted: ,

496 The Maritime Continent of Southeast Asia has faced widespread and ubiquitous fires the past few
 497 decades, due to expanding agriculture, urban development, economic growth, and changes in the base
 498 climatology that induce drought [Center, 2005; Dennis et al., 2005; van der Werf et al., 2008; Taylor,
 499 2010]. These fires contribute the major fraction of the atmospheric aerosol burden during the dry season
 500 [Cohen, 2014]. However, these fires are unique: they are relatively low in radiative power and temperature,
 501 yet cover a massive net surface area, making their statistics and extent hard to characterize from remote
 502 sensing. Yet, their total emissions are very high and they dominate the aerosol optical depth (AOD) and
 503 PM_{2.5} levels over thousands of kilometers [Field et al., 2009; Nakajima et al., 1999]. Due to their
 504 widespread nature, fires in this region are geospatially coherent in their timing and geography, although
 505 individually they burn for different lengths of time, as a function of localized precipitation and soil
 506 moisture, and global circulation patterns such as El-Nino [Cohen, 2014; Wooster et al., 2012; Hansen,
 507 2008].

508 A comprehensive previous attempt to study aerosol height over Southeast Asia was performed by
 509 Lee et al. [2016]. They used the total The Cloud-Aerosol Lidar with Orthogonal Polarization (CALIOP)
 510 profile, but were not specific about how they cleared or accounted for high ice clouds that frequently found
 511 in this part of the world. They also used day-time data without considering the issues of solar reflection and
 512 backscatter [Winker et al., 2013]. Furthermore, they used satellite derived single scattering albedo (SSA)
 513 approximated by each pass, although this product has been shown to be highly error-prone over Southeast
 514 Asia [Rogers et al., 2009; Hostetler, 2008]. This work did not address how the spatially-disparate individual
 515 path measurements from CALIOP, sampling both fire plume and non fire plume pixels jointly, as compared
 516 to the approach used by Cohen [2014] and Cohen et al. [2017]. While there were a few other attempts to
 517 use CALIOP over this region, there has not been any direct local validation of the CALIOP product by
 518 other LIDAR related instruments [Sugimoto et al., 2014a]. The only comparisons made so far have been
 519 model-based validation studies [Campbell et al., 2013].

520 This work describes a new approach to comprehensively sample the vertical distribution of smoke
 521 aerosols, by first using decadal scale measurements of AOD from the Multi-angle Imaging
 522 SpectroRadiometer [MISR] satellite [Cohen, 2014], and then separating the smoke impacted regions by
 523 the magnitude of the measured variability. During the 2006 El-Nino enhanced burning, one of the 2 largest
 524 such events over the past 15-year measurement record, this approach yields a much higher vertical aerosol
 525 height than the traditional random sampling approach. A simple plume-rise model [Achtemeier et al., 2011;
 526 Briggs, 1965] using reanalysis meteorology [Kalnay et al., 1996] and measured fire properties was found to
 527 underestimate the measured heights. However, the model could be improved to match the median heights
 528 by increasing the measured fire radiative power [Sessions et al., 2011; Sofiev et al., 2012], implying that the
 529 measured fires may be underestimated in terms of their strength, or that there are missing fires. However,
 530 the top and bottom heights of the measured plume still cannot be reproduced. The data shows that an
 531 improved representation of both localized convective transport and the aerosol direct and semi-direct

Deleted: to provide additional spatial resolution to go with each pass

Deleted: but which

Deleted: The

Deleted: using

Deleted: have also been done, but without any

Deleted: 5

Deleted: , or have used

Deleted: s

Deleted: to

Deleted: e

Deleted: the CALIOP measurements

544 effects [Ekman et al., 2007; Wang, 2007] are required to make further improvements. It is hoped that these
545 results will provide insight to those working on understanding the strong 2015-2016 El-Nino conditions.

546 2. Methods

547 2.1 Geography

548 This work is focused on the Maritime Continent, a sub region of Southeast Asia (8°S to 8°N, 95°E
549 to 125°E) (Figure 1) that experiences wide-spread and highly emitting fires on a yearly basis during the
550 local dry season (starting in August/September and proceeding continuously through October/November).
551 The combined magnitude of the fires produces effectively a single massive smoke plume in the atmosphere,
552 that covers much of the region, extending thousands of kilometers [Cohen, 2014]. These wide spread fires
553 are due to anthropogenic clearing of rainforest and agriculture [Cohen et al., 2017; Dennis et al., 2005; van
554 der Werf et al., 2008; Taylor, 2010; Miettinen et al., 2013; Langmann et al., 2009]. Over this region, during
555 the dry season, the removal of aerosols is quite slow, leading to the overall properties of the plume being
556 relatively consistent over space and time [Cohen, 2014]. Therefore, the overall properties of the smoke
557 plume, when correctly bounded in space and time, can be robustly statistically related to the overall
558 properties of individual fires, and daily measurements of AOD from the MISR satellite (Figure 1) [Cohen,
559 2014].

560 In 2006, the El-Nino conditions led to an enhanced drought, with subsequent fires lasting from
561 September through November. To ensure that this event is uniquely and completely analyzed, data from
562 September 3rd through November 9th is ultimately used (more details are given in Figure 2 and Figure 3a,
563 which are defined later). The region in (Figure 1) with the EOF larger than 2.2 (Bjornsson and Venegas,
564 1997; Cohen et al., 2017), calculated from the measured MISR AOD, comprising the boundary of the
565 source regions (over land) and downwind regions (over both land and sea). This analytically provides a
566 holistic representation in space and time of the impact of individual fires on the large-scale structure of the
567 aerosol plume, hence allowing a comprehensive sampling of the vertical distribution of the smoke,
568 including all sources, both observed and obscured by clouds (very common in this region), and aged
569 aerosols downwind from their initial sources.

570 2.2 Measurements

571 The CALIOP instrument is an active lidar, quantifying the vertically resolved atmospheric
572 backscatter strength at 532 nm and 1064 nm (a reasonable approximation of the vertical profile of
573 aerosols), and and polarization at 532 nm. The combination of these measurements allows additionally for
574 an indication of particle size (large or small) and cloud or aerosol [Winker et al., 2003]. Specifically, we use
575 the backscatter at 532nm and the vertical feature mask (vertical resolution 30m below 8.2km and 60m from
576 8.2km to 20.2km, horizontal resolution 1/3km) [Hostetler et al., 2006]. Clouds are identified and removed,
577 and night time data only is used, to avoid issues of cloud contamination and solar reflectance [Winker et al.,
578 2013].

579 Since the width of each pass is narrow, they are not spatially representative in general. However,
580 given the relative consistency of the plume as a whole, samples constrained within the plume's spatial

Deleted:

Deleted: o

Deleted: only

Formatted: Superscript

Formatted: Superscript

Deleted: October

Formatted: Font:Bold

Deleted: of

Deleted: larger than 2.2

Deleted: is

Deleted: net of the

Deleted: CALIPSO is an active lidar that quantifies both the vertically resolved atmospheric backscatter strength

591 extent, taken on the same day, are statistically representative of the smoke plume as a whole [Cohen, 2014].
 592 This approach is not only consistent with [Winker et al., 2013], but actually takes the results one step
 593 further, but relaxing the uniform “horizontal box size”, and instead re-focusing it in a scientifically
 594 homogenous and representative manner, consisting of a much larger number of measurements, allowing for
 595 improved statistical representation.

596 The extinction-weighted top (10% vertically integrated height), middle-upper (30% vertically
 597 integrated height), median (50% vertically integrated height), middle-lower (70% vertically integrated
 598 height), and bottom (90% vertically integrated height) are computed for each individual measurement, with
 599 the values retained if the aerosol is not in the stratosphere (assumed to be 15km) (Supplemental Figure 1).
 600 The data is then aggregated first by day, and secondly by geography, either into the fire-impacted region, or
 601 non fire-impacted region, based on (Figure 1) [Cohen, 2014]. The aggregated set of measurements is used
 602 to compute probability densities and statistics, demonstrating the vast difference over the fire-impacted and
 603 non-fire impacted regions (Figures 3a, 3b). The vertical heights both significantly higher and less variable
 604 ($p < 0.01$) over the fire region than the non-fire region, inclusively from September 3rd through November
 605 9th.

606 Measurements of aerosol optical depth (AOD) [Kaufman et al., 2003], fire radiative power (FRP)
 607 and fire temperature (T_F) [Freeborn et al., 2014; Ichoku et al., 2008] are obtained from the MODIS
 608 instrument aboard both the TERRA and AQUA satellites. Version 5, level 2, swath-by-swath measurements,
 609 at daily resolution are use for AOD (best solution 0.55 micron), with a spatial resolution of 10km by 10km,
 610 and FRP/ T_F , with a spatial resolution of 1km by 1km. Given the prevalence of clouds in this region, the
 611 cloud-cleared products are used, leading to a possible low bias in the FRP/ T_F measurements, as well as
 612 some fires not measured at all [Cohen et al., 2017; Freeborn et al., 2014; Ichoku et al., 2008; Kahn et al.,
 613 2008; Kahn et al., 2007]. On the other hand, while some grids are contaminated, the sheer spatial distance
 614 of the plume and the fact that the overwhelming majority of atmospheric aerosols during this time of the
 615 year are due to fires, means that there is no observable bias in the overall statistics of the measured AOD
 616 [Cohen, 2014], as observed by looking at the spatially averaged MODIS AOD and statistics over the fire-
 617 constrained and non fire-constrained regions (Figure 2). The AOD is higher ($p < 0.01$) over the fire-
 618 constrained region, from September 3rd through November 9th, making the findings consistent with the
 619 approach employing the 12-years worth of MISR measurements, as well as the results from the CALIOP
 620 observations already discussed.

621 In terms of MODIS retrieval uncertainties over land, especially during fire events, there are two
 622 important issues to consider. The first is that under extremely high AOD conditions ($AOD > 2$), frequently
 623 aerosols are flagged/reclassified as clouds, which brings about a negative bias. This bias would lead to an
 624 even higher AOD over the fire plume region if it were properly handled, leading to an even larger
 625 difference between “fire region” and the “non-fire region”. The second is the error in the over-land retrieval
 626 can go as high as 15%. However, based on the results in (Figure 2 and Supplemental Figure 2), the
 627 difference between the “fire region” and the “non-fire region” is statistically sound even assuming the error

Deleted: 2
 Deleted: 2
 Deleted: with t
 Formatted: Superscript

Deleted: 10kmx10km
 Deleted: x

Deleted: 3
 Formatted: Superscript
 Formatted: Superscript
 Deleted:

Deleted: 3

is larger than 15%. It is also the reason why MISR was used for the initial definition of the two regions, since its ability to cloud clear is better than MODIS over this region [Kahn et al., 2010].

While there are many errors involved with using the satellite data, the errors in this case are sufficiently small as to not impact the analysis and results over Southeast Asia during the fire season (Cohen, 2014; Cohen et al., 2017). The AOD and certain surface products, when used to run models, have been found to compare in magnitude, spatial, and temporal extent, to various ground based surface and column measurements, such as from Aerosol Robotic Network [AERONET], the United States National Oceanic and Atmospheric Administration surface measurement network [NOAA], and other available air pollution networks. The data-driven models have been shown to lead to a reduction in the annualized RMS error as compared with the Intergovernmental Panel on Climate Change Representative Concentration Pathways [IPCC RCP] emissions scenarios by a factor of 2 to 8 against AERONET stations throughout Asia (Cohen and Wang, 2014). Furthermore, on a month-to-month basis, the results of the data-driven models have been shown to lead to a reduction in the RMS error by a factor of 1.8 and of an improvement in the coefficient of determination statistic [R^2] by a value of 0.2 to 0.3, when compared against the Global Fire Emissions Database [GFED] dataset (Cohen 2014; Cohen et al. 2017). Given these findings, it is reasonable to assume that the methodology is as reliable as anything else presently available, with respect to this work.

2.3 Plume Rise Model

A simple model is employed to simulate the height to which a parcel of air initially at the surface over the fire will rise, based on buoyancy, vertical, and horizontal advection (Supplement). The formulation requires information about the temperature and radiative power of the fire as well as local meteorology [Achtemeier et al., 2011; Briggs, 1965], and yields an idealized height to which aerosols emitted will rise. The buoyant plume rise is a thermodynamic approximation in nature and thus not as physically realistic as a large eddy approach, which solves the atmospheric fluid dynamical equations by parameterizing turbulence at the scale of tens of meters. However, it is less computationally expensive and more generalizable in the context of approximating the thousands of fires spread geographically over hundreds of thousands of square kilometers. On the other hand, it is more physically realistic than empirical relationships from multi-angle measurements [Sofiev et al., 2012], which have also been attempted, but show poor performance in Southeast Asia.

These relationships are efficiently solved using measurements of meteorological and fire properties, allowing them to be used as rapid parameterizations within regional or global models. However, there are errors associated with reconciling the different temporal and spatial scales of reanalysis meteorology, especially convection and associated transport. Secondly, cloud-cover in this region leads to both missing fires and low-bias in measurements of fire properties [Sofiev et al., 2012; Kaufman et al., 2003]. Third, the cloud-cover also leads to a heavier contribution of model results in the reanalysis meteorology. Finally, the effects of the optically thick aerosol plume's feedback on the radiative profile is

Deleted: are

Deleted: national

Deleted: statistic

Deleted: of

Formatted: Superscript

Deleted: against

Deleted: GDED

Deleted: Fire emissions

likely important, but beyond the scope of this work and hence not taken into consideration [Ekman et al., 2007; Wang, 2007].

3. Results and Discussion

3.1 Measured Aerosol Vertical Distribution

The fire-constrained monthly aggregated daily statistics of the measured vertical aerosol height from CALIPSO [Winker et al., 2003] is given in (Figure 3a), with the aggregated statistics from the October fire-maximum time and (the entirety of the fire season) over the fire-constrained region of the bottom, middle-lower, median, middle-upper, and top heights respectively: $1.68 \pm 1.55\text{km}$ ($1.49 \pm 1.58\text{km}$), $1.92 \pm 1.51\text{km}$ ($1.76 \pm 1.54\text{km}$), $2.19 \pm 1.50\text{km}$ ($2.04 \pm 1.52\text{km}$), $2.53 \pm 1.51\text{km}$ ($2.38 \pm 1.54\text{km}$), and $3.03 \pm 1.52\text{km}$ ($2.91 \pm 1.57\text{km}$) (Table 1). These results are supported by the statistical values of aerosol heights measured by the MPL station in Singapore throughout the period from September 1 to November 30, 2015 (Supplemental Figure 3), which are found to range from 1.6km to 2.4km. 2015 was selected to compare against ground-based lidar measurements, since there were none available from 2006, and 2015 was also a strong El-Nino year which impacted Singapore, including very large amounts of downwind aerosols arriving from burning sources. Overall, the close resemblance between these years allows inference from the results.

On the other hand, the non fire-constrained region's aggregated statistics of the measured vertical aerosol height is quite different (Figure 3b), with the respective bottom, middle-lower, median, middle-upper, and top heights during the October maximum-fire period being: $0.65 \pm 0.98\text{km}$, $0.93 \pm 0.98\text{km}$, $1.21 \pm 1.00\text{km}$, $1.53 \pm 1.02\text{km}$, and $1.98 \pm 1.08\text{km}$ (Table 1). The average aerosol height over the fire-constrained region is both much higher and more variable at every vertical level as compared to the non fire-constrained domain. This difference leads to 61(+6-10)% of the bottom of the smoke plume and 83(+8-11)% of the median of the smoke plume in the free troposphere during the October maximum; while 49(+7-9)% and 75(+12-12)% of the respective bottom and median of the aerosol loading is in the free troposphere over the entirety of the fire-season, over fire-constrained domain. On the other hand, only 17(+10-9)% of the median of the aerosol loading is located in the free troposphere over the non fire-constrained domain during the October maximum fire period. However, the variability is roughly constant at all levels over the fire-constrained region, while the variability increases with vertical level, over the non fire-constrained region. These results are based on more than 10,000 daily CALIOP measurements.

All three findings, higher average aerosol height, larger variance of height, and a consistent variance of height at all levels, are consistent with areas where most of the aerosol loading is due to surface fires. Firstly, the buoyancy from fires increases the expected height, with differences in buoyancy from different strength fires producing random variability in the measured heights. So long as the distribution of fire strength and meteorology do not differ too much from day-to-day, the variance in aerosol heights should also not vary much. On the other hand, over non fire-constrained regions, the major contribution to the vertical aerosol variability is convection, which is expected to increase in variability the higher one moves upwards from the surface.

Deleted: 2

Deleted: monthly aggregated statistics

Deleted:

Formatted: Font:Italic

Deleted: 68

Deleted: 9

Deleted: 92

Deleted: 5

Deleted: 17

Deleted: 3

Deleted: 50

Deleted: 8

Deleted: 5

Deleted:

Deleted:

Deleted: monthly

Deleted: 2

Formatted: Not Highlight

Formatted: Not Highlight

Deleted: , with 62% of

Formatted: Not Highlight

Formatted: Not Highlight

Formatted: Not Highlight

Deleted: ,

Deleted: while

736 Furthermore, the relatively constant variability across the heights in the fire-constrained region is
 737 consistent with a proposed radiative-stabilization effect. The extremely high measured AOD values found
 738 by MODIS [Kaufman *et al.*, 2003] over the fire-constrained domain (from 0.5 to 2.0, with most days over
 739 1.0), leads to observable surface cooling (Figure 2). Additionally, black carbon aerosols [BC] emitted from
 740 the fire, absorbs incoming solar radiation near the upper portion of the plume, providing a source of
 741 warming. This combination leads to additional stabilization of the atmosphere, and therefore reinforces the
 742 observed vertical aerosol distribution.

743 These results are thus consistent with the observed reduction in in-situ vertical processing over the
 744 regions downwind from the fire sources, but still within the fire-constrained plume region, where buoyancy
 745 from the fires and the self-stabilization effect seem to contribute more than random deep convection.
 746 However, over the non fire-constrained region, given the low AOD and lack of fires, both of these effects
 747 are not observed, and convection dominates, which is consistent with the less uniform vertical distribution.
 748 Given these clear and observed differences, only results from the fire-constrained region will be considered
 749 further.

750 A significant amount of aerosol mass exists in the free troposphere over this region. Assuming the
 751 measured boundary layer height can be represented by the range from 700m to 1300m, with a central value
 752 of 1000m (as observed in Singapore [Chew *et al.*, 2013]) and applied over the domain, the resulting total
 753 loading of aerosols over the boundary layer can be computed. This value, when applied over the entire
 754 geographical domain, the amount of measurements above the boundary layer in October is found to be
 755 [67.61,51]%, [80.70,61]%, [91.83,72]%, [96.92,83]%, and [99.97,94]% respectively of the bottom, lower-
 756 middle, median, upper-middle and top extinction. Although October is slightly more intense, the same
 757 pattern, just to a slightly lesser extent, is found throughout the entire season, with [56.49,40]%,
 758 [72.61,51]%, [87.75,63]%, [96.90,77]%, and [99.97,93]% of the measurements respectively of the bottom,
 759 lower-middle, median, upper-middle and top extinction. This is much higher than previous studies, which
 760 indicated most of the smoke remained within the boundary layer [Tosca *et al.*, 2011].

761 Analysis of the daily measured heights demonstrates 3 statistically unique days: October 11th, 15th
 762 and 22nd (Table 2). On the 11th, the top and upper-middle measurements fall within the top 15%, while the
 763 median measurements fall within the top 20% of the month's measurements, implying that the result is
 764 consistent with a deep, single layer, extending throughout the lower and middle free-troposphere. The 15th
 765 and 22nd, while not being as high in the middle-troposphere, also have little to no aerosol in the planetary
 766 boundary layer due to being more confined in the vertical, implying a narrow layer in the middle free-
 767 troposphere. These results are consistent with the measured aerosol layer being mostly in the free
 768 troposphere, a result that is not consistent with the measured FRP or meteorology, leading to two important
 769 implications. Firstly, the aerosol lifetime on these days will be considerably longer than models typically
 770 reproduce and the radiative forcing will be considerably more warming. Secondly, that typical modeling
 771 approach that fresh aerosols are mixed from the surface to the given top of the plume height is likely not

Deleted: 3

Deleted: By

Deleted: a

Deleted: that

Deleted: of

Deleted:

Formatted: Not Highlight

Deleted: is applied to the domain, then

Deleted: 62%

Deleted: 93

Formatted: Not Highlight

Formatted: Not Highlight

Deleted: 98

Formatted: Not Highlight

Formatted: Not Highlight

Deleted: 73%

Formatted: Not Highlight

Deleted: 83%

Formatted: Not Highlight

Formatted: Not Highlight

Formatted: Not Highlight

Deleted: of the total monthly respective measurements

Formatted: Not Highlight

Deleted:

Formatted: Not Highlight

Deleted: heights are located in the free troposphere

787 true here, which has implications for the ability of most models to be able to correctly capture the aerosol
788 loading.

789 On the remaining days, the measured heights are consistent on a daily average basis with relatively
790 uniform emissions, meteorology, and vertical buoyant rise. Although present, intense but heterogeneous
791 forcing impacting the vertical distribution, such as localized convection and aerosol cloud interactions are
792 generally not observed to bias the overall plume's properties. Only on October 11th, 15th, and 22nd, are there
793 higher heights or a narrower vertical structure, combined with no readily available explanation to be found
794 in the fire, AOD, or meteorological properties on these days. ~~This combination can only be explained by~~
795 ~~either a~~ clear change in the convection on those days, or some other phenomena not considered ~~in or~~
796 ~~otherwise represented by~~ the reanalysis meteorology. The robustness of this approach assures the validity of
797 ~~these results~~ over the region and time period ~~herein~~.

798 A comparison between the inverse model by Campbell et al. [2013; Supplemental Figure 6] and
799 this work's underlying Kalman Filter plus variance maximization ~~modeled fields~~, shows that ~~this new~~
800 ~~modeling approach~~ performs ~~better~~ during the biomass burning season, [Cohen, 2014; Cohen and Wang,
801 2014; Cohen et al., 2017]. Furthermore, the results found using the approach employed here, match well
802 with individual measurement campaigns done by Lin Neng-Hui, et al. [2013, 2014, etc.], and the AD-Net
803 measurement network [Sugimoto et al, 2014b], that have focused on observations from a small number of
804 on-the-ground lidar at multiple places within the Northern portion of Southeast Asia and Greater East Asia.
805 While the geographic regions are not identical and therefore cannot be used to directly validate the region
806 studied here, there is a sufficient amount of similarity, that there is some likelihood of overlap in the results.
807 Given these factors, we present the results here as the best available for use at this time, when targeting this
808 region of the world during the biomass burning season.

809 3.2 Measured Fire and Meteorological Properties

810 The daily aggregated measurements of fire radiative power (FRP) [Freeborn et al., 2014; Ichoku et
811 al., 2008] indicate there are 109395 actively burning 1kmx1km pixels in October 2006. However, filtering
812 for high confidence [Level 9] active fires, reduces this number to 6941 1kmx1km pixels. The respective
813 measurements have 10%, median, and 90% values of FRP of [115,300,975] W/m² for all fires and
814 [185,540,1495] W/m² for high confidence fires (**Table 3**). Overall, these values are much lower than FRP
815 measured over other intensely burning regions [Giglio et al., 2006]. However, the results are consistent
816 with the fact that fires in the Maritime Continent occur under relatively wet surface conditions, due to high
817 levels of mineral-soil moisture, extensive peat, and intermittent localized precipitation [Couwenberg et al.,
818 2010]. These results are based on more than 3000 daily MODIS fire hotspots and associated meteorological
819 measurements.

820 There is only one day, October 2nd, with a statistically high FRP (daily mean more than monthly
821 90% value), for high confidence fires. Similarly, there are two days, October 28th and 30th, with an
822 abnormally low FRP (daily mean less than monthly 15% value), for high confidence fires. None of these
823 days have a statistically abnormal fire vertical height distribution. However, October 28th and 30th both

Deleted: , indicating a likely

Deleted: captured

Deleted: considered

Deleted: inversely

Deleted: eir model

Deleted: considerably less

Deleted: well

Deleted: , which is the focus of this work

832 show a sizable increase in AOD over the fire constrained region, with the AOD more than 2 standard
833 deviations greater than the mean over the non fire constrained region, as compared to the period of time
834 from the 25th through the 27th. One consistent rationale is that there was large-scale precipitation event at
835 that time, which in turn both increased aerosol removal and wetting of the surface. This in turn led to lower
836 temperature and FRP and correspondingly higher aerosol emissions factor on these days. Overall, there is
837 no apparent impact of day-to-day variability of measured FRP driving observed variation in measured
838 aerosol heights, and hence only high confidence fire data is subsequently used.

839 To examine this hypothesis, the GPCP [Global Precipitation Climatology Project] One-Degree
840 Daily Precipitation Data Set of global precipitation has been employed to study the amount and duration of
841 rainfall over the fire-burning and non fire-burning regions [Huffman et al., 2012]. A spatial/temporal
842 analysis of this dataset, over both the Fire Region and the No-Fire region confirms this hypothesis
843 (Supplemental Figure 4) Supp. Overall, there was considerably lower rainfall over the Fire Region than
844 the No-Fire Region, however, on all days that there was a decrease in AOD and FRP over the Fire Region,
845 there was a heavy Rainfall at the same time, or one or two days before. The measurements have a
846 correlation coefficient of -0.39 with a corresponding $p < 0.01$. There is no other statistically significant
847 correlation found over any other combination of the regions with any other combination of rainfall.

848 The Modern-Era Retrospective Analysis for Research and Applications [MERRA] [Rienecker et
849 al., 2011] reanalysis meteorology is used for the horizontal and vertical wind, and vertical temperature
850 profile at each location where a fire is measured (Table 3). MERRA was chosen because it is based on
851 NASA satellite measurements, and thus should be more consistent with the measurements used here. With
852 the exceptions of October 5th and 20th, the horizontal wind is relatively calm $6.0 \pm 1.3\text{m/s}$. Also, throughout
853 the entire month, the vertical temperature gradient is relatively stable $-5.45 \pm 0.16\text{K/km}$, with only 7
854 individual fires occurring under unstable atmospheric conditions. Therefore, dynamical instability is not
855 expected to contribute greatly to the vertical distribution [Stone and Carlson, 1979]. Also, the role played
856 by the large-scale vertical wind is small $2.1 \pm 1.6\text{mm/s}$. Given the atmospheric stability and fire-controlled
857 buoyancy conditions, the plume rise model approach should offer a reasonable approximation of the aerosol
858 vertical distribution.

859 The approach used here relies upon the atmosphere being either stable or only minority non-stable.
860 However, in general in this part of the world, there are two reasons that would contribute to most fires
861 occurring under such conditions: firstly, that major instability would frequently lead to rain, fire
862 suppression, and aerosol wash-out; and secondly that the induced surface cooling and atmospheric heating
863 by the extensive aerosol layer itself would tend to increase the atmospheric stability. Such points are made
864 clear in terms of the major unaccounted for processes in the MERRA data at this resolution, being:
865 localized convection (due to the resolution), and the aerosol cooling and in-situ heating effects (not
866 incorporated into MERRA's underlying model). In theory the direct and semi-direct effect may be able to
867 be parameterized, but this would require a higher order model. Hence, since these conditions and effects are

Deleted: ing

Deleted: subsequently

Formatted: Font:Bold

not considered by the plume rise model, they therefore cannot be explanations for discrepancies in the modeled vertical distribution.

3.3 Modeled Aerosol Vertical Distribution

Applying the plume rise model, the aggregated daily statistics of the vertical aerosol height at the bottom, lower-middle, median, upper-middle, and top for the October fire-maximum time and (the entirety of the fire season) are 0.60km (0.41km), 1.14km (0.88km), 1.85km (1.40km), 2.87km (2.25km), and 4.99km (3.95km) respectively (Figure 4, Table 4). The mean of the daily median, lower-middle, and bottom modeled heights are consistently lower than the respective mean of the measured heights for the October fire-maximum time and (the entirety of the fire season) by 0.34km (0.64km), 0.78km (0.88km), and 1.08km (1.08km) respectively. The day-to-day differences between show that the model generally underestimates the measurements, with the minimum and maximum differences between the two both ranging from -0.92 km to 1.36km, -0.63 km to 2.20km, and -0.19 km to 3.02km, respectively. The upper-middle modeled height is about equal to measurements, with a mean difference for the October fire-maximum time and (the entirety of the fire season) of an underestimate of 0.34km over the October maximum to an overestimate of 0.13km through the entire fire season. The associated day-to-day variations are wide, but are roughly centered around zero, and vary from -1.22km to 1.06km. Finally, the top modeled heights are considerably higher than measurements, with an average overestimate for the October fire-maximum time and (the entirety of the fire season) being 1.96km and (1.04km) respectively. The day-to-day difference between the model and the measurements generally overestimates the measurements, with a value varying from -1.54 to 0.81km.

The model underestimates the height of the median through bottom of the plume, while simultaneously overestimating the top. First, this means that the model is not accounting for enough energy to obtain the average rise of the plume. At the same time, the modeled vertical spread is too large, implying other factors limit the height gain near the top of the plume while simultaneously enhance the height near the bottom. The results are consistent with one or both of the two hypothesized effects; first, that a low bias exists in the measured values of FRP [Kahn et al., 2007; Kahn et al., 2008], leading to insufficient buoyancy; and second, that in-situ stabilization occurs due to aerosol radiative cooling in the lower parts of the plume and aerosol radiative heating within the upper parts of the plume. This combination of factors is also consistent with the observed underestimate in measured FRP to match the median height, as well as the hypothesized complete non-detection of small fires [Kaufman et al., 2003]. There are also uncertainties in the MERRA reanalysis products, but given the large sample size and the narrowness of the MERRA distribution, the impact of these uncertainties is considerably smaller than changes in the FRP on the order of 10%.

A sensitivity analysis is used to quantify the effects of a low bias in FRP, by applying a constant multiplicative factor to the measured FRP for each fire, from 1.0 to 2.0 in steps of 0.1 (although only the results in steps of 0.2 are given in Table 4). Although there are also uncertainties associated with measured vertical wind and temperature structure, this is not considered (Table 3), since there is no way to couple

Deleted: ,
Deleted: an
Deleted: mean
Deleted:
Deleted:
Deleted: 48km
Deleted: 78km
Deleted: 07km
Deleted: , with a wide underestimate day-to-day
Deleted:
Deleted:
Deleted: from 1.91km to 1.11km.
Formatted: Highlight
Deleted: 0.03
Deleted: , and wide
Deleted: ,
Formatted: Not Highlight
Deleted: an overestimate of
Deleted: 97km
Formatted: Not Highlight
Deleted: an underestimate of
Deleted: 36km
Formatted: Not Highlight
Deleted: of
Deleted: 2
Deleted: , and a
Deleted: range from an overestimate of 3.96km to an underestimate of 0.44km
Formatted: Not Highlight
Deleted: .

932 meteorological effects at sub-grid scale, or otherwise not included in the reanalysis meteorology. The
 933 results are obtained by minimizing the root-mean square (RMS) difference between the daily measured and
 934 modeled heights, for each FRP scaling factor, at each of the middle-upper, median, and middle-lower
 935 levels. The respective best-fit enhancement factors over the October fire maximum (and the entire fire
 936 season) are **1.0 (1.0)** for middle-upper measurements, having an RMS error of 0.69km (0.66km), **1.2 (1.2)**
 937 for median measurements, having an RMS error of 0.78km (0.72km), and **1.6 (1.4)** for middle-lower
 938 measurements, having an RMS error of 0.92km (0.82km) (**Figure 4**).

939 Another source of uncertainty is due to the height of the boundary layer itself, which is also
 940 uncertain, due to both a lack of measurements, and a poor ability of reanalysis and other global scale
 941 products to simulate the boundary layer, especially in this part of the world. As discussed before, the model
 942 was run in a sensitivity mode, assuming 3 different average boundary layer heights. The results for the
 943 middle-upper, median, and middle-lower levels best fit values over the October fire maximum (and the
 944 entirety of the fire season) are enhancements of 1.0, 1.4, and 1.8 and (1.0, 1.1, and 1.5) respectively for a
 945 boundary layer height of 1300m and 1.0, 1.3, and 1.6 and (1.0, 1.1, and 1.4) for a boundary layer height of
 946 700m. These results show that while this factor is highly important in terms of modulating the magnitude of
 947 the best-fitting FRP scaling factor, that similar biases still exist, where the model is reasonably good at
 948 reproducing the upper-middle levels of the plume, but is strongly biased in the median and middle-lower
 949 levels of the plume. Additionally, the larger values of the RMS error at the two more extreme boundary
 950 layer heights, lend further support to the initial supposition that overall, the boundary layer height, on
 951 average throughout the fire region, lies within these boundaries.

952 Although there is no single best-fit FRP scaling factor, a reasonable fit of the model, based on
 953 measured values from the middle-lower to the middle-upper plume levels can be obtained by using an
 954 appropriate FRP enhancement. The results establish that current plume rise models can reproduce the
 955 median vertical plume height over Southeast Asia by increasing the FRP by 20%, a finding consistent with
 956 FRP generally underestimated over this region. By changing the FRP enhancement from 0% to **60%**, the
 957 central **40% of the aerosol plume's vertical extent can be** modeled, although the top and bottom heights of
 958 the plume cannot be reproduced. Additionally, the modeled plume is widely spread as compared to the
 959 narrowness of the measured plume. Unfortunately, rectifying these limitations will likely require the use of
 960 a more complex modeling approach and improvement of measured fire data.

961 There are additional errors associated with the non-complete complexity of the models employed.
 962 The models do not capture the contribution of atmospheric stabilization due to both the direct and semi-
 963 direct aerosol effects. Furthermore, these models do not take into account the impacts of localized
 964 convection. However, the majority of other works that employ regional and global models use this exact
 965 same methodology, and hence they also neglect these same small-scale phenomena in terms of
 966 communication between the chemistry, radiation, and the meteorology.

Formatted: Not Highlight
Deleted: (RMS=0.94km)
Deleted: ,
Deleted: (
Deleted: =
Deleted: 81
Deleted: ,
Deleted: 2
Deleted: 0
Formatted: Not Highlight
Deleted:
Formatted: Not Highlight
Deleted: (RMS=0.74km)
Deleted: Table

Deleted:
Deleted: the results produce a
Deleted: better
Deleted: to
Deleted: than using the model without any
Deleted: -
Deleted: 100
Deleted: height of the plume can be

4. Conclusions

This work quantifies the significant present-day underestimation of the vertical distribution of aerosols over the Maritime Continent during an El-Nino influenced fire season, by introducing a new method to appropriately constrain the measurements over the geographical region of the aerosol plume. While this was a large-scale fire event, it was very special, because it occurred throughout the month of October, whereas typically the wet-season arrives sometime within the middle of the month. As such, the wetness of the soil and the large-scale meteorological flow, were both different this year from a more typical year. As a result, the measured heights over the constrained region are found to be higher than previously thought, with about 61(+6-10)% of the bottom of the aerosol layer and 83(+8-11)% of the median of the aerosol layer being in the free troposphere during the October maximum; while correspondingly 49(+7-9)% and 75(+12-12)% of the total aerosol height and the median of the aerosol plume, are found in the free troposphere during the entirety of the fire-season. In this case, they can be advected thousands of kilometers and have more impact on the atmospheric and climatic systems.

Additionally, over the fire-constrained region, the vertical variability of the plume is found to be uniform throughout its height, implying that it is controlled mostly by local forcing, such as the buoyancy released by fires, localized convection, and aerosol/radiative feedbacks, such as the direct and semi-direct effects.

Application of a plume-rise model showed that there was an overall low bias against measured heights, which is consistent with the FRP being underestimated in this region of the world due to large-scale cloud cover. It was also determined that measured vertical heights are more narrowly confined than model simulations. Applying a robust sensitivity analysis found that the middle-lower through middle-upper extent of the plume can be reproduced if an appropriate (although changing) enhancement is applied to the FRP ranging from 1.0*FRP to 1.6*FRP over the maximum period of the fire season, through the month of October (and from 1.0*FRP to 1.4*FRP over the fire season as a whole, for most of September, all of October, and the first third of November). Hence, the variable FRP enhancement factor approach can allow for improved modeling of the height statistics for the middle-upper to middle-lower extent of the plume.

However, it is not possible to reproduce either the top or bottom of the measured heights, the knowledge of which is important to constrain the impacts of long-range transport and aerosol-climate interactions. Nor is it possible to reproduce the narrow spread of the measured heights. The results are consistent with the general understanding of current model shortcomings, which in addition to the underestimated FRP values, will also need to be addressed. Hence, the current community-wide dependence on FRP measurements for vertical aerosol modeling may lead to flaws in our being able to successfully model the distribution.

The results have been found to be robust over a region that behaves roughly uniformly over thousands of kilometers and includes regions both near and far from the source of the fires. Since there are only a few days that have relatively unique aerosol and meteorological properties over the period studied, the results support the most important aspect of improving the aerosol heights will be newer modelling

Deleted: comprehensively

Deleted: 62% of aerosols found in the free troposphere,

Deleted: where

Deleted: 2

Deleted: 0

Deleted: with

Deleted: 2

Deleted: the best fit-value

1032 approaches and improvements that will be able to resolve local-scale forcing, such as deep convection,
1033 aerosol/radiation interactions, and aerosol-cloud interactions. Secondly, the biased underestimation of FRP
1034 is also an important point to improve the aerosol height modeling, especially under conditions where
1035 cloudiness occurs or the measured AOD levels are very high. These errors are exacerbated over regions
1036 where large-scale precipitation is very low or where there is substantial aerosol/cloud intermixing. In all
1037 cases, until these model and measurement improvements are made, there is expected to be a significant
1038 underestimation of the aerosol loadings and radiative forcing distribution regionally, and to some extent
1039 globally. It is hoped that in the interim, the community will adapt a variable enhancement of FRP in tandem
1040 with measurement-constrained boundaries of smoke plumes, as a way to more precisely reproduce the
1041 statistics of the vertical aerosol distribution.

1042 **Acknowledgements:**
1043 We would like to acknowledge the PIs of the NASA MODIS, MISR, and CALIPSO projects for providing
1044 the data. The work was supported by the Chinese National Young Thousand Talents Program (Project
1045 ~~74110-41180002~~), the Chinese National Natural Science Foundation (Project 74110-41030028), and the
1046 ~~Guangdong Provincial Young Talent Support Fund (Project 74110-42150003)~~.

Deleted: 74110-52601113

Formatted: Not Highlight

Formatted: Not Highlight

Deleted: and the Chinese Ministry of Science and Technology (Project 74110-41110002)

Deleted: .

1051 **References:**

1052 Achtemeier, G., S. Goodrick, Y. Liu, F. Garcia-Menendez, Y. Hu, and M. Odman, (2011). Modeling smoke

1053 plume-rise and dispersion from Southern United States prescribed burns with daysmoke.

1054 *Atmosphere*, 2, 358-388.

1055 Bjornsson, H. and Venegas, S, (1997). A Manual for EOF and SVD Analyses of Climate Data. Department

1056 of Atmospheric and Oceanic Sciences and Centre for Climate and Global Change Research, Tech.

1057 rep., McGill University, Technical Report, 1997.

1058 Bond, T. C., D.G. Streets, K.F. Yarber, S.M. Nelson, J.H. Woo, and Z. Klimont. (2004). A technology-based

1059 global inventory of black and organic carbon emissions from combustion, *J. Geophys. Res.*, 109,

1060 D14203, doi:10.1029/2003JD003697.

1061 Briggs, G. A. (1965). A plume rise model compared with observations. *Journal of the Air Pollution Control*

1062 *Association*, vol. 15, no. 9, pp. 433–438.

1063 Burnett, R., A. Pope, M. Ezzati, C. Olives, S. Lim, S. Mehta, H. Shin, G. Singh, B. Hubbell, M. Brauer, R.

1064 Anderson, K. Smith, J. Balmes, N. Bruce, H. Kan, F. Laden, A. Pruss-Ustun, M. Turner, S. Gapstur,

1065 R. Diver, and A. Cohen. (2014) An Integrated Risk Function for Estimating the Global Burden of

1066 Disease Attributable to Ambient Fine Particulate Matter Exposure, *Environ Health Perspect*;

1067 doi:10.1289/ehp.1307049.

1068 Campbell, J.R., Reid, J.S., Westphal, D.L., Zhang, J.L., Tackett, J.L., Chew, B.N., Welton, E.J., Shimizu,

1069 A., Sugimoto, N., Aoki, K., Winker, D.M. (2013) Characterizing the vertical profile of aerosol

1070 particle extinction and linear depolarization over Southeast Asia and the Maritime Continent: The

1071 2007–2009 view from CALIOP, *Atmospheric Research*, 122, March 2013, 520–543,

1072 <http://dx.doi.org/10.1016/j.atmosres.2012.05.007>.

1073 Chew, B. N., J.R. Campbell, S.V. Salinas, C.W. Chang, J.S. Reid, E.J. Welton, and S.C. Liew. (2013).

1074 Aerosol particle vertical distributions and optical properties over Singapore. *Atmospheric*

1075 *Environment*, 79, 599-613.

1076 Chung, C. E., V. Ramanathan and D. Decremer. (2012) Observationally constrained estimates of

1077 carbonaceous aerosol radiative forcing, *Proc. Natl. Acad. Sci. U.S.A.*,

1078 doi:10.1073/pnas.1203707109.

1079 Cohen, J. B. and Prinn, R. G. (2011). Development of a fast, urban chemistry metamodel for inclusion in

1080 global models, *Atmos. Chem. Phys.*, 11, 7629–7656, doi:10.5194/acp-11-7629-2011.

1081 Cohen, J. B. (2014) Quantifying the occurrence and magnitude of the Southeast Asian fire climatology.

1082 *Environmental Research Letters*, 9(11), 114018.

1083 Cohen, J. B., Lecoecur, E., and Hui Loong Ng, D. (2017) Decadal-scale relationship between measurements

1084 of aerosols, land-use change, and fire over Southeast Asia, *Atmos. Chem. Phys.*, 17, 721-743,

1085 doi:10.5194/acp-17-721-2017.

1086 Cohen, J. B. and Wang C (2014) Estimating Global Black Carbon Emissions Using a Top-Down Kalman

1087 Filter Approach. *J. Geophys. Res.*, doi:10.1002/2013JD019912.

1088 Colarco, P., M. Schoeberl, B. Doddridge, L. Marufu, O. Torres, and E. Welton. (2004) Transport of smoke
1089 from Canadian forest fires to the surface near Washington, D.C.: Injection height, entrainment, and
1090 optical properties, *J. Geophys. Res.*, 109, D06203, doi:10.1029/2003jd00424.

1091 Couwenberg, J., R. Dommain, and H. Joosten, H. (2010). Greenhouse gas fluxes from tropical peatlands in
1092 south-east Asia. *Global Change Biology*, 16: 1715–1732. doi:10.1111/j.1365-2486.2009.02016.

1093 Delene, D. J. and J.A. Ogren (2002) Variability of aerosol optical properties at four North American
1094 surface monitoring sites, *J. Atmos. Sci.*, 59(6), 1135–1150.

1095 Dennis, R. A., J. Mayer, G. Applegate, U. Chokkalingam, C.J.P. Colfer, I. Kurniawan, and T.P. Tomich.
1096 (2005). Fire, people and pixels: linking social science and remote sensing to understand underlying
1097 causes and impacts of fires in Indonesia. *Human Ecology*, 33(4), 465-504.

1098 Dubovik, O., A. Smirnov, B.N. Holben, M.D. King, Y.J. Kaufman, T.F. Eck and I Slutsker. (2000)
1099 Accuracy assessments of aerosol optical properties retrieved from Aerosol Robotic Network
1100 (AERONET) Sun and sky radiance measurements. *J. Geophys. Res.*, 105(D8), 9791-9806.

1101 Ekman, A., A. Engstrom and C. Wang. (2007). The effect of aerosol composition and concentration on the
1102 development and anvil properties of a continental deep convective cloud, *Q. J. Roy. Meteor. Soc.*,
1103 133B(627), 1439-1452.

1104 Ekman, A. M. L., M. Hermann, P. Gross, J. Heintzenberg, D. Kim, and C. Wang. (2012). Sub-micrometer
1105 aerosol particles in the upper troposphere/lowermost stratosphere as measured by CARIBIC and
1106 modeled using the MIT-CAM3 global climate model, *J. Geophys. Res.*, 117, D11202,
1107 doi:10.1029/2011JD016777.

1108 Field, R. D., G.R. van der Werf, S.P.P. Shen. (2009) Human amplification of drought-induced biomass
1109 burning in Indonesia since 1960. *Nature Geosci.*, 10.1038/ngeo443.

1110 Freeborn, P. H., M.J. Wooster, D.P. Roy and M.A. Cochrane. (2014). Quantification of MODIS fire
1111 radiative power (FRP) measurement uncertainty for use in satellite-based active fire characterization
1112 and biomass burning estimation, *Geophys. Res. Lett.*, 41, 1988–1994, doi:10.1002/2013GL59086.

1113 Giglio, L., I. Csiszar and C.O. Justice. (2006) Global distribution and seasonality of active fires as observed
1114 with the Terra and Aqua MODIS sensors. *J. Geophys. Res.*, doi:10.1029/2005JG000142.

1115 Hansen, M. C. (2008). Humid tropical forest clearing from 2000 to 2005 quantified by using multitemporal
1116 and multiresolution remotely sensed data. *Proc. Natl. Acad. Sci. USA*, 105, 9439–9444.

1117 Hostetler, C., Hair, J., Liu, Z.Y., Ferrare, R., Harper, D., Cook, A., Vaughan, M., Trepte, C., Winker, D.
1118 (2008) Validation of CALIPSO Lidar Observations Using Data From the NASA Langley Airborne
1119 High Spectral Resolution Lidar (Retrieved from:
1120 <https://ntrs.nasa.gov/archive/nasa/casi.ntrs.nasa.gov/20080014234.pdf>)

1121 Hostetler, C, Z. Liu, J. Reagan, M. Vaughan, D. Winker, M. Osborn, W. Hunt, K. Powell, and C. Trepte.
1122 (2006). CALIOP Algorithm Theoretical Basis Document—Part 1: Calibration and Level 1 Data
1123 Products. *Doc. PC-SCI* 201.

1124 [Huffman, G.J., Bolvin, D.T., and Adler, R.F. \(2012\) last updated 2012: GPCP Version 1.2 1-Degree Daily](#)
 1125 [\(1DD\) Precipitation Data Set. WDC-A, NCDC, Asheville, NC. Data set accessed November 1, 2017](#)
 1126 [at http://www.ncdc.noaa.gov/oa/wmo/wdcametncdc.html.](http://www.ncdc.noaa.gov/oa/wmo/wdcametncdc.html)
 1127 Ichoku, C., L. Giglio, M. Wooster and L. Remer. (2008). Global characterization of biomass-burning
 1128 patterns using satellite measurements of fire radiative energy. *Remote Sensing of Environment* 112.6,
 1129 2950-2962.
 1130 [Kahn, R.A., Gaitley B.J., Garay M.J., Diner, D.J., Eck, T.F., Smirnov, A., and Holben, B.N. \(2010\)](#)
 1131 [Multiangle Imaging SpectroRadiometer global aerosol product assessment by comparison with the](#)
 1132 [Aerosol Robotic Network. J. Geophys. Res. Atmos. 115, D23209, doi:10.1029/2010JD014601](#)
 1133 Kahn, R.A., Chen, Y., Nelson, D.L., Leung, F.Y., Li, Q.B., Diner, D.J., and Logan, J.A. (2008). Wildfire
 1134 smoke injection heights: Two perspectives from space. *Geophys. Res. Lett.*, 35, L04809,
 1135 doi:10.1029/2007GL032165.
 1136 Kahn, R.A., Li, W.H., Moroney, C., Diner, D.J., Martonchik, J.V., and Fishbein, E. (2007). Aerosol source
 1137 plume physical characteristics from space-based multiangle imaging. *J. Geophys. Res.*, 112,
 1138 D11205, doi:10.1029/2006JD007647, 2007
 1139 Kalnay et al. (1996). The NCEP/NCAR 40-year reanalysis project. *Bull. Amer. Meteor. Soc.*, 77, 437-470.
 1140 Kaufman, Y. J., C. Ichoku, L. Giglio, S. Korontzi, D.A. Chu, W.M. Hao, and C.O. Justice. (2003). Fire and
 1141 smoke observed from the Earth Observing System MODIS instrument--products, validation, and
 1142 operational use. *International Journal of Remote Sensing*, 24(8), 1765-1781.
 1143 Kim, D., C. Wang, A.M.L. Ekman, M. C. Barth, and P. Rasch. (2008) Distribution and direct radiative
 1144 forcing of carbonaceous and sulfate aerosols in an interactive size-resolving aerosol-climate model,
 1145 *J. Geophys. Res.*, 113, D16309, doi:10.1029/2007JD009756.
 1146 Lamarque, J. F. (2010). Historical (1850–2000) gridded anthropogenic and biomass burning emissions of
 1147 reactive gases and aerosols: methodology and application. *Atmos. Chem. Phys.*, doi:10.5194/acp-10-
 1148 7017-2010.
 1149 Langmann, B., B. Duncan, C. Textor, J. Trentmann, and G.R. van der Werf. (2009). Vegetation fire
 1150 emissions and their impact on air pollution and climate. *Atmospheric Environment*, 43(1), 107-116.
 1151 Lee, J., Hsu, N.C., Bettenhausen, C., Sayer, A.M., Seftor, C.J., Jeong, M.J., Tsay, S.C., Welton, E.J., Wang,
 1152 S.H., Chen, W.N. (2016) Evaluating the Height of Biomass Burning Smoke Aerosols Retrieved
 1153 from Synergistic Use of Multiple Satellite Sensors over Southeast Asia, *Aerosol and Air Quality*
 1154 *Research*, 16: 2831–2842 doi:10.4209/aaqr.2015.08.0506
 1155 Leung, F.Y.T., J.A. Logan, R. Park, E. Hyer, E. Kasischke, D. Streets, and L. Yurganov. (2007) Impacts of
 1156 enhanced biomass burning in the boreal forests in 1998 on tropospheric chemistry and the sensitivity
 1157 of model results to the injection height to emissions. *J. Geophys. Res.*, 112, D10313,
 1158 doi:10.1029/2006JD008132.

Deleted: .

1160 Lin, N. H., A.M. Sayer, S.H. Wang, A.M. Loftus, T.C. Hsiao, G.R. Sheu, and S. Chantara. (2014).
 1161 Interactions between biomass-burning aerosols and clouds over Southeast Asia: Current status,
 1162 challenges, and perspectives. *Environmental Pollution*, 195, 292-307.
 1163 Martin, V.M., R.A. Kahn, J.A. Logan, R. Paugam, M. Wooster, and C. Ichoku. (2012). Space-based
 1164 observational constraints for 1-D fire smoke plume-rise models. *Journal of Geophysical Research:*
 1165 *Atmospheres (1984–2012)*, 117(D22).
 1166 Miettinen, J., E. Hyer, A.S. Chia, L.K. Kwok, and S.C. Liew, S. C. (2013). Detection of vegetation fires
 1167 and burnt areas by remote sensing in insular Southeast Asian conditions: current status of knowledge
 1168 and future challenges. *International journal of remote sensing*, 34(12), 4344-4366.
 1169 Ming, Y., V. Ramaswamy and G. Persad. (2010) Two opposing effects of absorbing aerosols on global-
 1170 mean precipitation. *Geophysical Research Letters* 37.13.
 1171 Nakajima, T., A. Higurashi, N. Takeuchi and J.R. Herman (1999). Satellite and ground-based study of
 1172 optical properties of 1997 Indonesian Forest Fire aerosols. *Geophys. Res. Lett.*,
 1173 10.1029/1999GL900208.
 1174 Petersen, W. and S. Rutledge. (2001). Regional Variability in Tropical Convection: Observations from
 1175 TRMM. *J. Climate*, 14, 3566–3586.
 1176 Petrenko, M., R.A. Kahn, M. Chin, A.J. Soja, T. Kucsera, and Harshvardhan. (2012) The use of satellite-
 1177 measured aerosol optical depth to constrain biomass burning emissions source strength in the global
 1178 model GOCART, *J. Geophys. Res.*, doi:10.1029/2012JD01787.
 1179 Rienecker, M.M., M.J. Suarez, R. Gelaro, R. Todling, J. Bacmeister, E. Liu, M.G. Bosilovich, S.D.
 1180 Schubert, L. Takacs, G.-K. Kim, S. Bloom, J. Chen, D. Collins, A. Conaty, and A. da Silva (2011).
 1181 MERRA: NASA's Modern-Era Retrospective Analysis for Research and Applications. *J. Climate*,
 1182 24, 3624-3648, doi:10.1175/JCLI-D-11-00015.1
 1183 Rogers, R.R., Hostetler, C.A., Ferrare, R.A., Hair, J.W., Obland, M.D., Cook, A.L., Harper, D.B., Swanson,
 1184 A.J. (2009) Validation of CALIOP Aerosol Backscatter and Extinction Profile Products Using
 1185 Airborne High Spectral Resolution Lidar Data (Retrieved from:
 1186 http://cimss.ssec.wisc.edu/calipso/meetings/cloudsat_calipso_2009/Posters/Rogers.pdf)
 1187 Schuster, G. L., O. Dubovik, B. Holben and E. Clothiaux. (2005) Inferring black carbon content and
 1188 specific absorption from Aerosol Robotic Network (AERONET) aerosol retrievals, *J. Geophys.*
 1189 *Res.*, 110, D10S17, doi:10.1029/2004JD004548.
 1190 Sessions, W. R., H.E. Fuelberg, R.A. Kahn, and D.M. Winker. (2011). An investigation of methods for
 1191 injecting emissions from boreal wildfires using WRF-Chem during ARCTAS. *Atmospheric*
 1192 *Chemistry and Physics*, 11(12), 5719-5744.
 1193 Sofiev, M., T. Ermakova, and R. Vankevich. (2012). Evaluation of the smoke-injection height from
 1194 wildland fires using remote-sensing data. *Atmos. Chem. Phys.*, vol. 12, no. 4, pp. 1995–2006.
 1195 Stone, P. and J. Carlson. (1979). Atmospheric Lapse Rate Regimes and Their Parameterization. *J. Atmos.*
 1196 *Sci.*, 36, 415–423.

1197 Sugimoto, N., Nishizawa T., Shimizu A., Matsui I., Jin Y. (2014a) Characterization of aerosols in East Asia
1198 with the Asian dust and aerosol lidar observation network (AD-Net) *Proc. SPIE* 9262 92620K
1199 Sugimoto, N., Shimizu, A., Nishizawa, T., Matsui, I., Jin, Y., Khatri, P., Irie, H., Takamura, T., Aoki, K.,
1200 Thana, B. (2014b) Aerosol characteristics in Phimai, Thailand determined by continuous
1201 observation with a polarization sensitive Mie–Raman lidar and a sky radiometer, *Environmental*
1202 *Research Letters*, 10, 6.
1203 Tao, W.K., J.P. Chen, Z.Q. Li, C. Wang, and C.D. Zhang. (2012) The Impact of Aerosol on convective
1204 cloud and precipitation. *Rev. Geophys.*, 50, RG2001, doi:10.1029/2011RG000369.
1205 Taylor, D. (2010). Biomass burning, humans and climate change in Southeast Asia. *Biodiversity and*
1206 *conservation*, 19(4), 1025-1042.
1207 Tosca, M. G., J.T. Randerson, C.S. Zender, D.L. Nelson, D.J. Diner, and J.A. Logan (2011), Dynamics of
1208 fire plumes and smoke clouds associated with peat and deforestation fires in Indonesia, *J. Geophys.*
1209 *Res.*, 116, D08207, doi:10.1029/2010JD015148.
1210 Tsigaridis, K., N. Daskalakis, M. Kanakidou, P.J. Adams, P. Artaxo, R. Bahadur, Y. Balkanski, S.E.
1211 Bauer, N. Bellouin, A. Benedetti, T. Bergman, T.K. Berntsen, J.P. Beukes, H. Bian, K.S.
1212 Carslaw, K. S., M. Chin, G. Curci, T. Diehl, R.C. Easter, S.J. Ghan, S.L., Gong, A. Hodzic, C.R.
1213 Hoyle, T. Iversen, S. Jathar, J.L. Jimenez, J.W. Kaiser, A. Kirkevag, D. Koch, H. Kokkola, Y.H.
1214 Lee, G. Lin, X. Liu, C. Luo, X. Ma, G.W. Mann, N. Mihalopoulos, J.J. Morcrette, J.F. Müller, G.
1215 Myhre, S. Myriokefalitakis, N.L. Ng, D. O'Donnell, J.E. Penner, L. Pozzoli, K.J. Pringle, L.M.
1216 Russell, M. Schulz, J. Sciare, O. Seland, D.T. Shindell, S. Sillman, R.B. Skeie, D. Spracklen, T.
1217 Stavrakou, S.D. Steenrod, T. Takemura, P. Tiitta, S. Tilmes, H. Tost, T. van Noije, P.G. van Zyl, K.
1218 von Salzen, F. Yu, Z. Wang, Z. Wang, R.A. Zaveri, H. Zhang, K. Zhang, Q. Zhang, and X.
1219 Zhang, X. (2014) The AeroCom evaluation and intercomparison of organic aerosol in global
1220 models, *Atmos. Chem. Phys.*, 14, 10845-10895, doi:10.5194/acp-14-10845-2014.
1221 Urbanski, Shawn (2014) Wildland fire emissions, carbon, and climate: Emission factors, *Forest Ecology*
1222 *and Management*, 317, 51–60.
1223 van der Werf, G. R. (2010). Global fire emissions and the contribution of deforestation, savanna, forest,
1224 agricultural, and peat fires (1997–2009). *Atmos. Chem. Phys.*, 10.5194/acp-10-11707-2010.
1225 van der Werf, G. R., J. Dempewolf, S.N. Trigg, J.T. Randerson, P.S. Kasibhatla, L. Giglio, and R.S DeFries.
1226 (2008). Climate regulation of fire emissions and deforestation in equatorial Asia. *Proceedings of the*
1227 *National Academy of Sciences*, 105(51), 20350-20355.
1228 Wang, C. (2013) Impact of anthropogenic absorbing aerosols on clouds and precipitation: A review of
1229 recent progresses, *Atmos. Res.*, 122, 237-249.
1230 Wang, C. (2007). Impact of direct radiative forcing of black carbon aerosols on tropical convective
1231 precipitation, *Geophys. Res. Lett.*, 34, L05709, doi:10.1029/2006GL028416.
1232 Winker, D. M., J. Pelon, and M.P. McCormick (2003), The CALIPSO mission: Spaceborne lidar for
1233 observation of aerosols and clouds, *Proc. SPIE*, **4893**, 1–11.

Formatted: Font:Italic

Formatted: Font:(Default) Cambria

1234 [Winker, D. M., Tackett, J. L., Getzewich, B. J., Liu, Z., Vaughan, M. A., and Rogers, R. R.: The global 3-D](#)
1235 [distribution of tropospheric aerosols as characterized by CALIOP, Atmos. Chem. Phys., 13, 3345-](#)
1236 [3361, <https://doi.org/10.5194/acp-13-3345-2013>, 2013](#)▼
1237 Woodward J. L. (2010). *Estimating the Flammable Mass of a Vapour Cloud: A CCPS Concept Book*, John
1238 Wiley & Sons, ISBN 0470935359, 9780470935354.
1239 Wooster, M. J., G.L.W. Perry and A. Zoumas. (2012) Fire, drought and El Niño relationships on Borneo
1240 (Southeast Asia) in the pre-MODIS era (1980–2000), Biogeosciences, 9, 317-340, doi:10.5194/bg-9-
1241 317-2012.

Deleted: .

Table 1: Statistical summary of measured CALIPSO smoke plume heights in the El-Nino Season of 2006, at different percentiles of extinction height (top/Z=10%, middle-upper/ Z=30%, median/Z=50%, middle-lower/Z=70%, and bottom/Z=90%). *The numbers in normal print correspond to the data during the maximum of the fire season in October, while those numbers in (italics) correspond to the entire fire season from September 3rd through November 9th. All data is further divided into the subset of the Maritime Continent impacted by smoke (FIRE), and not impacted by smoke (NO-FIRE) (Figure 1).* “MEAN” is the average, “STD” is the standard deviation, and percentages XX% are the corresponding distribution’s percentiles.

	bottom [km]	middle-lower [km]	median [km]	middle-upper [km]	top [km]
FIRE 5%	0.18 (0.17)	0.35 (0.35)	0.56 (0.57)	0.85 (0.77)	1.27 (1.14)
FIRE 10%	0.25 (0.22)	0.48 (0.46)	0.74 (0.68)	1.06 (1.02)	1.50 (1.47)
FIRE 15%	0.30 (0.26)	0.58 (0.52)	0.88 (0.77)	1.24 (1.13)	1.64 (1.60)
FIRE 50%	1.35 (0.98)	1.58 (1.33)	1.81 (1.61)	2.18 (2.00)	2.77 (2.60)
FIRE 85%	2.73 (2.59)	2.90 (2.73)	3.11 (2.91)	3.35 (3.15)	3.70 (3.67)
FIRE 90%	3.14 (2.90)	3.29 (3.13)	3.44 (3.32)	3.66 (3.57)	4.09 (4.26)
FIRE 95%	4.19 (4.25)	4.38 (4.48)	4.70 (5.08)	5.56 (5.56)	5.65 (6.02)
FIRE MEAN	1.68 (1.49)	1.92 (1.76)	2.19 (2.04)	2.53 (2.38)	2.91 (3.03)
FIRE STD	1.58 (1.55)	1.54 (1.51)	1.52 (1.50)	1.54 (1.51)	1.57 (1.52)
NO-FIRE 5%	0.16	0.33	0.48	0.60	0.70
NO-FIRE 10%	0.19	0.38	0.55	0.68	0.87
NO-FIRE 15%	0.21	0.42	0.59	0.77	1.12
NO-FIRE 50%	0.31	0.57	0.83	1.25	1.76
NO-FIRE 85%	1.16	1.64	2.01	2.36	2.85
NO-FIRE 90%	1.65	1.98	2.27	2.60	3.05
NO-FIRE 95%	2.22	2.45	2.73	2.99	3.41
NO-FIRE MEAN	0.97	0.98	1.00	1.02	1.08
NO-FIRE STD	0.65	0.93	1.21	1.53	1.98

Table 2: Summary of measured (CALIPSO) smoke plume heights **over the entire fire season from September 3rd to November 9th 2006**, for days that are statistical outliers. **The values here correspond to having a mean value more than 85% of less than 15% in bold, or a mean value from 80% to 85% or from 15% to 20% in regular text.** The levels are given as a percentile of extinction height over the subset of the Maritime Continent impacted by smoke (fire-constrained), based on **the** MISR observations (**Figure 1**).

	bottom (90% Extinction) [km]	middle-lower (70% Extinction) [km]	median (50% Extinction) [km]	middle-upper (30% Extinction) [km]	top (10% Extinction) [km]
October 11th	2.29	2.54	3.26	4.11	4.93
October 15th	1.85	2.20			
October 22nd	2.55	2.85	2.95		

Deleted: in October

Deleted: ,

Formatted: Superscript

Formatted: Superscript

Deleted: mean (>85% or <15%) of all data

Deleted: mean (>80% or <20%) of all data

Formatted Table

Deleted: FIRE

Deleted: FIRE

Deleted: FIRE

Table 3: Statistics of measured fire properties (FRP and T_F), for all measured fires (**ALL**) and level 9 confidence fires (**L9**) and MERRA meteorological properties (T_A , v , U , dT/dz) corresponding to the geographic locations of **L9**. All data is constrained by the boundaries of the fire extent, and is applicable to results from the Maximum of the fire season corresponding to October 2006 (Figure 1). The distribution's percentile is given as "**XX%**", the mean and standard deviation are given as "**MEAN**" and "**STD**". Note that there were no observed fires of **L9** on the following dates: 17th, 22nd, 23rd, 24th, 25th, 26th, 27th, 29th, 31st.

	FRP ALL [W/m ²]	FRP L9 [W/m ²]	T_F ALL [K]	T_F L9 [K]	T_A L9 [K]	V L9 [mm/s]	U L9 [m/s]	dT/dz L9 [K/km]
5%	95.	140.	370.	410.	296.0	0.2	4.1	-5.25
10%	115.	185.	390.	445.	296.4	0.4	4.4	-5.27
15%	130.	230.	400.	480.	296.6	0.6	4.5	-5.28
50%	300.	540.	535.	725.	298.4	1.5	6.0	-5.43
85%	775.	1240.	910.	1275.	301.1	4.1	7.4	-5.65
90%	975.	1495.	1070.	1525.	301.5	4.6	7.7	-5.69
95%	1290.	1855.	1335.	1850.	302.1	5.6	8.1	-5.75
Mean	510.	920.	702.	1029.	298.7	2.1	6.0	-5.44
Std	720.	1340.	573.	1057.	2.0	1.6	1.3	0.16

Deleted: Monthly s

Deleted: in

Table 4: Statistics of the modeled fire heights corresponding to the maximum fire season of October and the (Entire fire season). All values are computed using level 9 confidence fires (L9) and MERRA meteorology (T_A , v , U , dT/dz) at the corresponding geographic locations, with the daily average boundary layer assumed to be 1000m. Sensitivity tests are shown with their respective weighting factor (1.2, 1.4, 1.6, 1.8, or 2.0) applied to the measured FRP. The modeled heights are given by percentile from the bottom (5%) to the top (95%), while the mean and standard deviation are given as “MEAN” and “STD”. Note that the model was not run on the following days, during which there were no observed L9 fires: September 13th, 14th, 15th, 16th, 17th, 27th, October 17th, 22nd, 23rd, 24th, 26th, 27th, and 31st, and November 2nd, 9th, 14th, 16th through 28th, 30th.

	FRP(x1.0) [km]	FRP(x1.2) [km]	FRP(x1.4) [km]	FRP(x1.6) [km]	FRP(x1.8) [km]	FRP(x2) [km]
5%	0.41 (0.26)	0.44 (0.30)	0.48 (0.33)	0.53 (0.35)	0.56 (0.38)	0.60 (0.41)
10%	0.60 (0.41)	0.67 (0.45)	0.73 (0.49)	0.80 (0.53)	0.85 (0.57)	0.91 (0.61)
15%	0.75 (0.55)	0.83 (0.61)	0.91 (0.66)	0.98 (0.72)	1.05 (0.77)	1.12 (0.82)
30%	1.14 (0.88)	1.28 (0.98)	1.40 (1.07)	1.52 (1.16)	1.63 (1.25)	1.74 (1.33)
50%	1.85 (1.40)	2.07 (1.58)	2.27 (1.73)	2.47 (1.88)	2.65 (2.02)	2.82 (2.15)
70%	2.87 (2.25)	3.23 (2.52)	3.54 (2.76)	3.84 (3.01)	4.12 (3.23)	4.38 (3.43)
85%	4.21 (3.29)	4.66 (3.67)	5.11 (4.02)	5.53 (4.35)	5.87 (4.64)	6.22 (4.92)
90%	4.99 (3.95)	5.54 (4.40)	6.08 (4.80)	6.58 (5.21)	6.97 (5.56)	7.41 (5.87)
95%	6.10 (5.25)	6.79 (5.86)	7.43 (6.39)	7.76 (6.83)	8.16 (7.22)	8.61 (7.57)
Mean	2.41 (1.94)	2.69 (2.17)	2.96 (2.38)	3.21 (2.58)	3.44 (2.77)	3.67 (2.95)
Std	1.98 (1.76)	2.21 (1.96)	2.42 (2.15)	2.62 (2.33)	2.81 (2.50)	2.99 (2.65)

Figure 1: Map of Maritime Continent. The smoke plume impacts the sub-region contained within the dashed lines, or the so-called **fire-constrained** region. On the other hand, the region outside of the dashed lines is the so-called **non fire-constrained** region. The colors on the plot correspond to the intensity of the variance, as explained in Cohen [2014]. The plot is based on a variance maximization technique applied to the measurements from all MISR overpasses from 2000 through 2014 (Cohen, 2014). Note that in this part of the world 1 degree of latitude or longitude is approximately 100km, leading to a fire-impacted region over 2500km across.

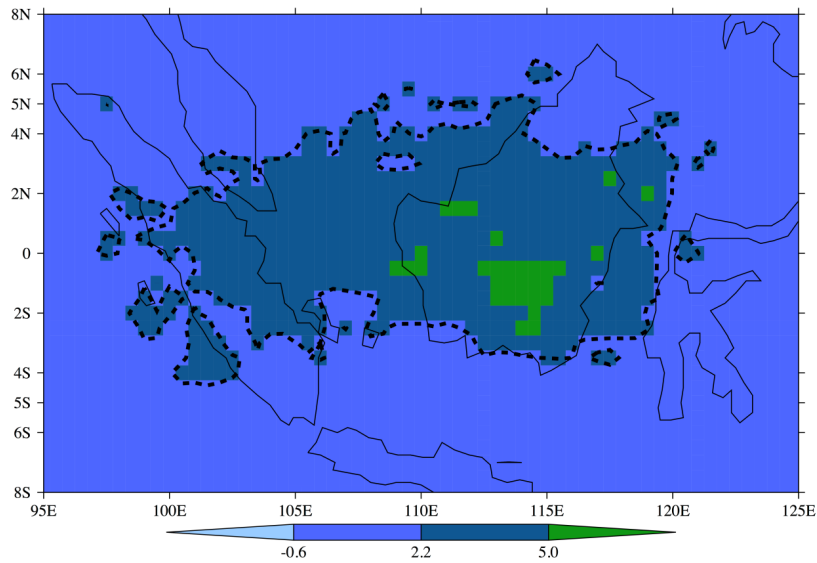
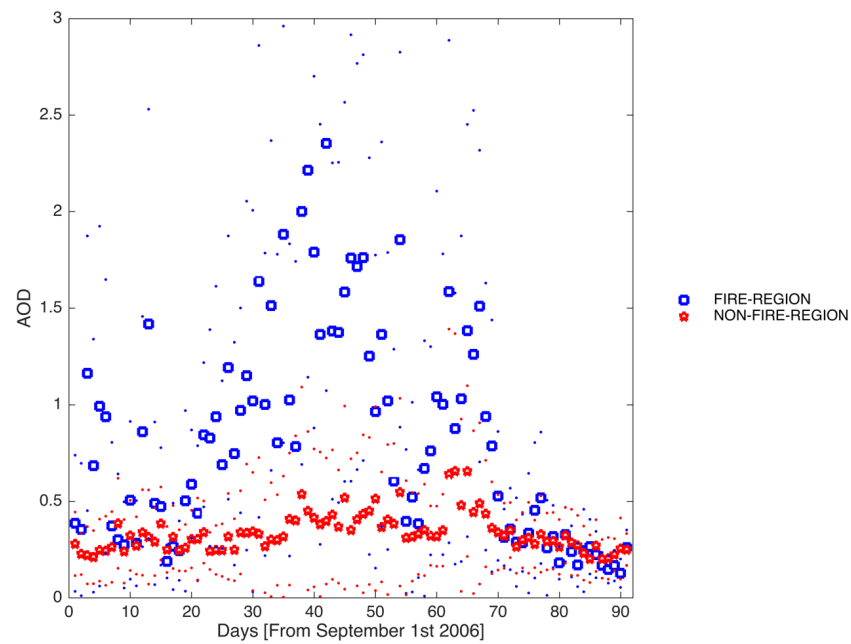
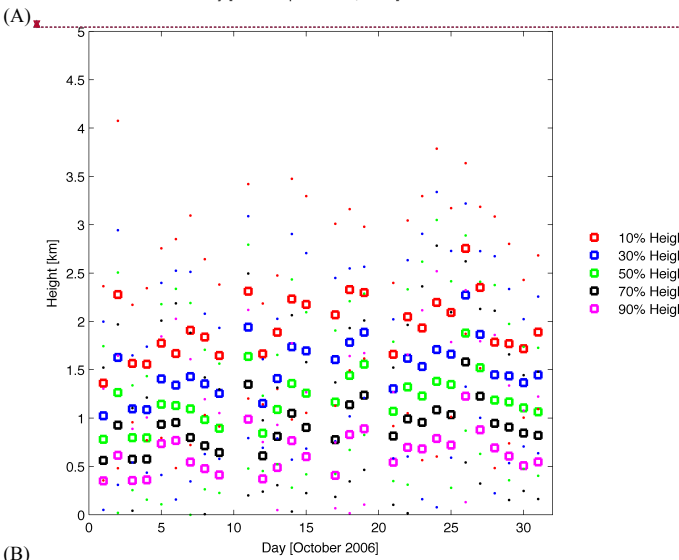
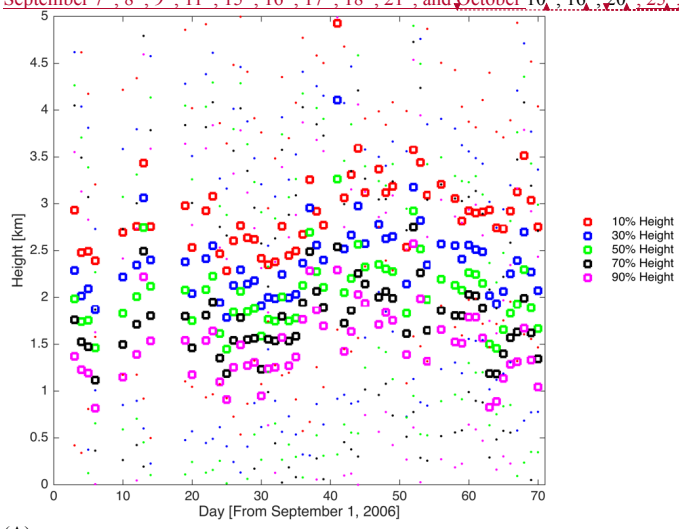


Figure 2: Time series of daily averaged measured AOD over the fire-constrained regions of the Maritime Continent [blue], and the non fire-constrained regions of the Maritime Continent [red], as given in **Figure 1**. Circles are computed daily mean values, while dots are computed daily standard deviation bands. Note that this figure contains the daily data from September 1, 2006 through November 30th, 2006.



Formatted: Font:(Default) Times New Roman, 10 pt, Font color: Text 1

Figure 3a, 3b: Time series of measured CALIPSO extinction heights over the fire constrained (A) and non fire-constrained (B) regions as given **Figure 1**. Note that for the fire constrained region, the analysis (and hence the data) has been extended for the period from September 3rd through November 9th. For both plots, the dots correspond to the height of the column integrated backscatter at: 10% [red] (top), 30% [dark blue], 50% [yellow], 70% [black], and 90% [light blue] (bottom). The circles are computed daily means, while dots are the computed daily standard deviation bands. There was no measurement over the region on September 7th, 8th, 9th, 11th, 15th, 16th, 17th, 18th, 21st, and October 10th, 16th, 20th, 25th, and 27th.



Deleted: 2

Deleted: 2

Formatted: Superscript

Formatted: Superscript

Deleted: the

Deleted: and

Deleted: .

Formatted: Superscript

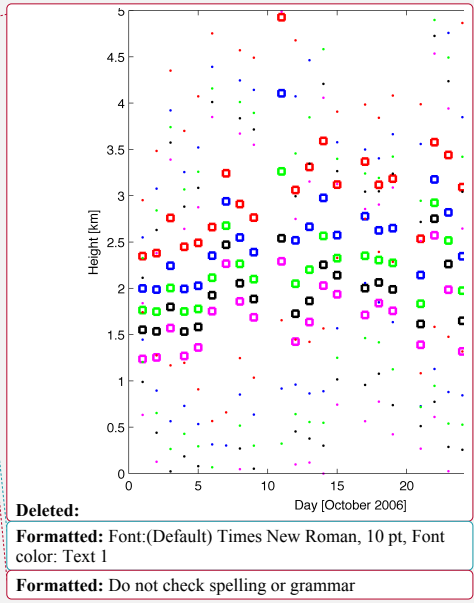
Formatted: Superscript

Formatted: Superscript

Formatted: Superscript

Formatted: Superscript

Formatted: Superscript

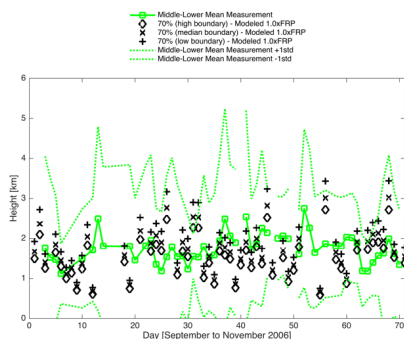
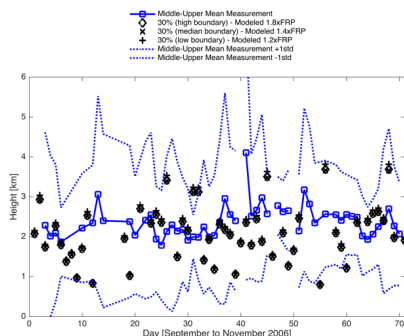
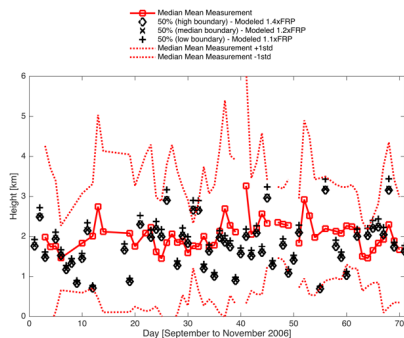


Deleted:

Formatted: Font:(Default) Times New Roman, 10 pt, Font color: Text 1

Formatted: Do not check spelling or grammar

Figure 4: Time series of measured extinction height levels for the median heights (red circles and line) with their corresponding ± 1 standard deviation range (red dotted line), and respective middle-upper (blue), and middle-lower (yellow), are given below. The best fitting modeled heights for the median daily boundary layer height of 1000m are given as black x's, and are found to be respective FRP enhancements of 1.0, 1.2, and 1.4. The best fitting modeled heights for the low daily boundary layer height of 700m are given as black +s, and are found to be respective FRP enhancements of 1.0, 1.1, and 1.2. The best fitting modeled heights for the high daily boundary layer height of 1300m are given as black o's, and are found to be respective FRP enhancements of 1.0, 1.4, and 1.8.



Deleted: Figure 3: Time series of daily averaged measured AOD over the fire-constrained regions of the Maritime Continent [blue], and the non fire-constrained regions of the Maritime Continent [red], as given in Figure 1. Circles are computed daily mean values, while dots are computed daily standard deviation bands. - (... [121])

Deleted: measured extinction heights

Formatted: Font:(Default) Times New Roman, 10 pt, Font color: Text 1

Deleted: PDFs (20% and 80% values are stars and mean values are given by lines) of the

Deleted: for

Deleted: median (red),

Deleted: green

Deleted: levels

Deleted: are given as 0% FRP enhancement (solid black line) (best fit for middle-upper measurements), 20% FRP enhancement (dashed black line) (best fit for median measurements), and 100% FRP enhancement (dotted black line) (best fit for the middle-lower measurements)

Formatted: Font:(Default) Times New Roman, 10 pt, Font color: Text 1

Formatted: Font:(Default) Times New Roman, 10 pt, Font color: Text 1

Formatted: Font:(Default) Times New Roman, 10 pt, Font color: Text 1

Formatted: Plain Text

Deleted: -

Formatted: Font:

Formatted: Font:(Default) Times New Roman, 10 pt, Bold, Font color: Text 1

Formatted: Not Highlight

Formatted: Highlight

Formatted: Not Highlight

Supplement:

Detailed Methodology

The buoyancy flux parameter (F_B) **Equation A1** is a function of the temperature difference between the air (T_A) and the fire (T_F), the vertical motion of air (v) and the size of the fire, d (here always measured at 1km^2 in this work).

$$F_B = gv \frac{d^2}{4} \left(\frac{T_F - T_A}{T_A} \right)$$

(A1)

The buoyancy flux parameter has been found empirically to demonstrate whether the plume rise is buoyancy or momentum dominated. Under stable atmospheric conditions [Stone and Carlson, 1979], where the atmospheric lapse rate is ($L_A = \frac{\Delta T}{\Delta Z} < -5$), for a buoyancy dominated plume, (defined as where the difference between T_A and T_F is given in **Equation A2b1**), the plume rise height (Δh) is given by **Equation A2b2**, where (U) is the horizontal wind magnitude.

$$(T_F - T_A) > 0.01958 T_F \sqrt{v}$$

(A2b1)

$$\Delta h = 2.4 \left(\frac{F_B}{0.02U} \right)^{1/3}$$

(A2b2)

Whereas, for a momentum dominated plume (where the difference between T_A and T_F is less than the right hand side of **Equation A2b1**), the height rise is given by **Equation A2b3**.

$$\Delta h = 1.5 \left(\frac{v^2 d^2 T_A}{\frac{4}{T_F} \sqrt{0.02U}} \right)^{1/3}$$

(A2b3)

On the other hand, under unstable atmospheric conditions (where $L_A > -5$), and where the plume rise is buoyancy dominated, the plume rise height is given by either **Equation A2b4** when $F_B > 55$ or **Equations A2b5, A2b6** when $F_B < 55$ [Woodward, 2010].

$$X^* = 14 F_B^{\frac{5}{8}}$$

(A2b4)

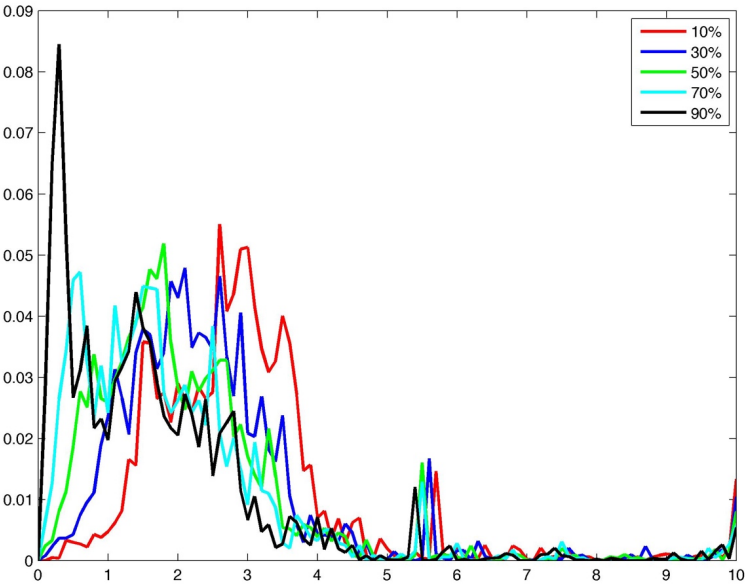
$$X^* = 34 F_B^{\frac{2}{5}}$$

(A2b5)

$$\Delta h = 1.6 \frac{F_B^{\frac{1}{3}} (3.5 X^*)^{\frac{2}{3}}}{U}$$

(A2b6)

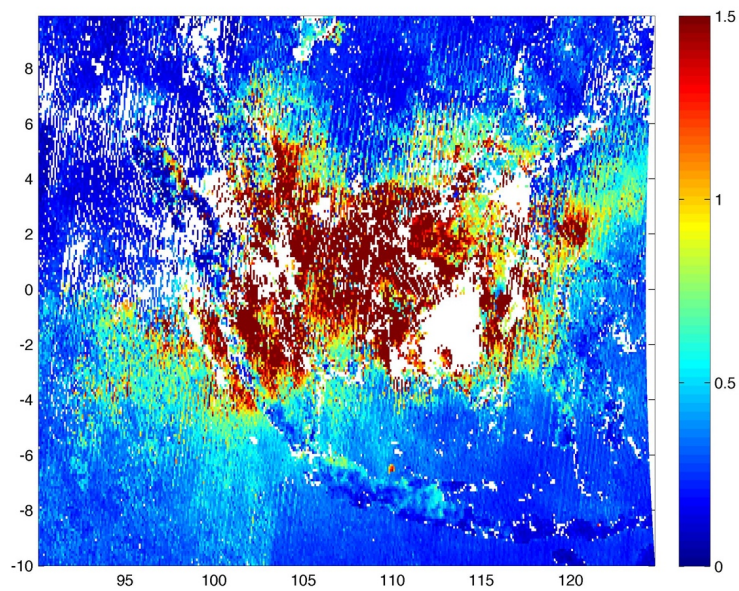
1507 **Supplemental Figure 1:** PDFs (x-axis is the height in km, and the y-axis is the probability distribution) of
1508 the monthly aggregated backscatter heights of the 10% [red] (top), 30% [dark blue], 50% [yellow], 70%
1509 [light blue], and 90% [black] levels. Note that there were no measurements on the 10th, 16th, and 20th.



1510
1511

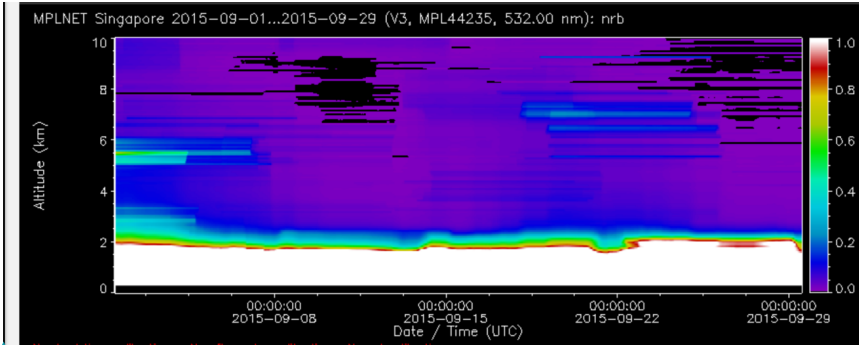
1512 **Supplemental Figure 2:** Map of the monthly averaged MODIS AOD over the Maritime Continent. The
1513 day-to-day statistics are given in **Figure 2**. Regions in white have 0 valid AOD measurements throughout
1514 the entire time period, due to cloud cover.

Deleted: 3

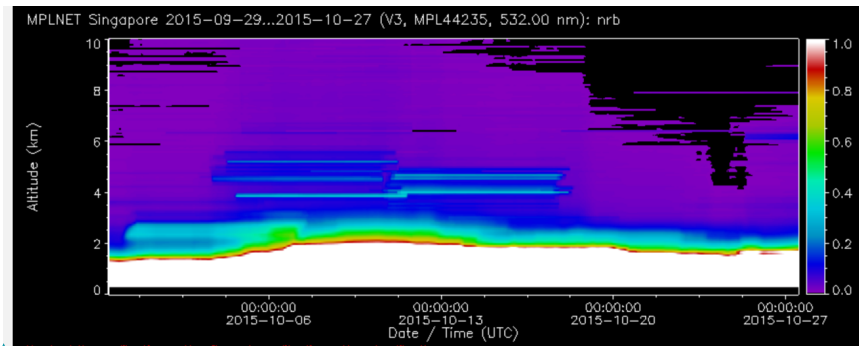


1515
1516
1517

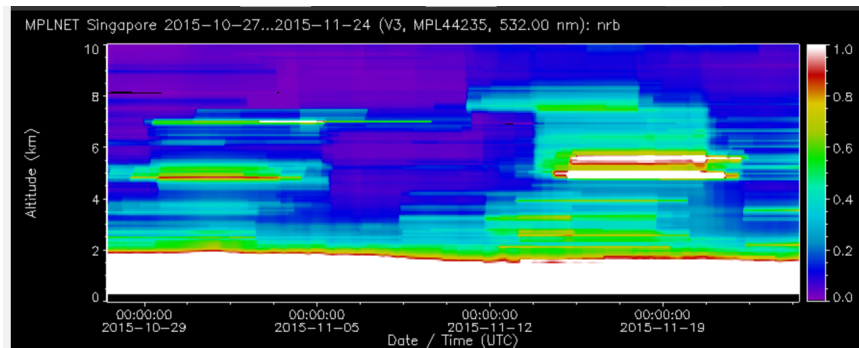
Supplemental Figure 3: Statistical average of the aerosol heights measured by the Singapore MPL station from September 1 to November 30, 2015. This year was chosen since it is another El-Nino influenced high fire year, and has a somewhat similar physical, meteorological, and geographic aerosol extent as 2006.



Formatted: Font:(Default) Times New Roman, 10 pt, Font color: Text 1

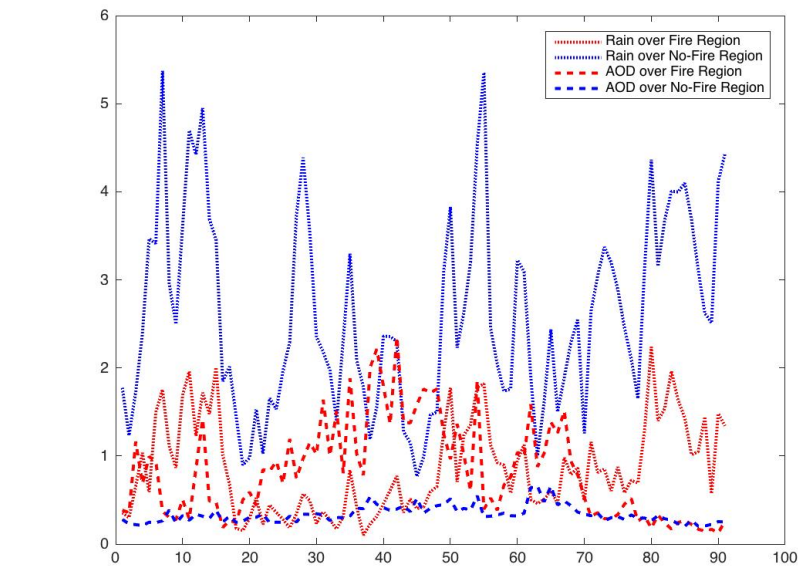


Formatted: Font:(Default) Times New Roman, 10 pt, Font color: Text 1



Formatted: Font:(Default) Times New Roman, 10 pt, Font color: Text 1

Supplemental Figure 4: Time Series of Precipitation data from GPCP (dotted line) and AOD (dashed line) from MODIS, averaged on a daily-basis over both the Fire Region (Red) and the No-Fire Region (Blue), from September 1 to November 30.



Formatted: Font:(Default) Times New Roman, 10 pt, Font color: Text 1

Page 21: [1] Deleted	Microsoft Office User	05/03/2018 3:52 PM
Page 31: [2] Deleted	Microsoft Office User	08/01/2018 12:59 PM
(
Page 31: [2] Deleted	Microsoft Office User	08/01/2018 12:59 PM
(
Page 31: [3] Formatted	Microsoft Office User	08/01/2018 1:00 PM
Font:Bold		
Page 31: [3] Formatted	Microsoft Office User	08/01/2018 1:00 PM
Font:Bold		
Page 31: [3] Formatted	Microsoft Office User	08/01/2018 1:00 PM
Font:Bold		
Page 31: [4] Deleted	Microsoft Office User	23/10/2017 2:33 PM
The numbers in normal print correspond to the subset of the Maritime Continent impacted by smoke (FIRE) , and not impacted by smoke (NO-FIRE) during the October maximum in fires , while the numbers in <i>(italics)</i> correspond to the impacted by smoke (FIRE) throughout the entire fire season from September 3rd through November 9th , based on MISR observations		
Page 31: [4] Deleted	Microsoft Office User	23/10/2017 2:33 PM
The numbers in normal print correspond to the subset of the Maritime Continent impacted by smoke (FIRE) , and not impacted by smoke (NO-FIRE) during the October maximum in fires , while the numbers in <i>(italics)</i> correspond to the impacted by smoke (FIRE) throughout the entire fire season from September 3rd through November 9th , based on MISR observations		
Page 31: [5] Formatted Table	Microsoft Office User	23/10/2017 2:35 PM
Formatted Table		
Page 31: [6] Formatted	Microsoft Office User	23/10/2017 3:34 PM
Font:Italic		
Page 31: [6] Formatted	Microsoft Office User	23/10/2017 3:34 PM
Font:Italic		
Page 31: [7] Formatted	Microsoft Office User	23/10/2017 3:34 PM
Font:Italic		
Page 31: [8] Formatted	Microsoft Office User	23/10/2017 3:31 PM
Font:Italic		
Page 31: [9] Formatted	Microsoft Office User	23/10/2017 3:11 PM
Font:Italic		
Page 31: [10] Formatted	Microsoft Office User	23/10/2017 3:34 PM
Font:Italic		
Page 31: [10] Formatted	Microsoft Office User	23/10/2017 3:34 PM
Font:Italic		

Page 31: [11] Formatted	Microsoft Office User	23/10/2017 3:34 PM
Font:Italic		
Page 31: [12] Formatted	Microsoft Office User	23/10/2017 3:30 PM
Font:Italic		
Page 31: [13] Formatted	Microsoft Office User	23/10/2017 3:11 PM
Font:Italic		
Page 31: [14] Formatted	Microsoft Office User	23/10/2017 3:35 PM
Font:Italic		
Page 31: [14] Formatted	Microsoft Office User	23/10/2017 3:35 PM
Font:Italic		
Page 31: [15] Formatted	Microsoft Office User	23/10/2017 3:34 PM
Font:Italic		
Page 31: [16] Formatted	Microsoft Office User	23/10/2017 3:30 PM
Font:Italic		
Page 31: [17] Formatted	Microsoft Office User	23/10/2017 3:11 PM
Font:Italic		
Page 31: [18] Formatted	Microsoft Office User	23/10/2017 3:05 PM
Font:Italic		
Page 31: [19] Formatted	Microsoft Office User	23/10/2017 3:35 PM
Font:Italic		
Page 31: [19] Formatted	Microsoft Office User	23/10/2017 3:35 PM
Font:Italic		
Page 31: [20] Formatted	Microsoft Office User	23/10/2017 3:33 PM
Font:Italic		
Page 31: [21] Formatted	Microsoft Office User	23/10/2017 3:30 PM
Font:Italic		
Page 31: [22] Formatted	Microsoft Office User	23/10/2017 3:10 PM
Font:Italic		
Page 31: [23] Formatted	Microsoft Office User	23/10/2017 3:04 PM
Font:Italic		
Page 31: [24] Formatted	Microsoft Office User	23/10/2017 3:35 PM
Font:Italic		
Page 31: [24] Formatted	Microsoft Office User	23/10/2017 3:35 PM
Font:Italic		
Page 31: [25] Formatted	Microsoft Office User	23/10/2017 3:33 PM
Font:Italic		
Page 31: [26] Formatted	Microsoft Office User	23/10/2017 3:29 PM

Font:Italic

Page 31: [27] Formatted	Microsoft Office User	23/10/2017 3:10 PM
-------------------------	-----------------------	--------------------

Font:Italic

Page 31: [28] Formatted	Microsoft Office User	23/10/2017 3:00 PM
-------------------------	-----------------------	--------------------

Font:Italic

Page 31: [28] Formatted	Microsoft Office User	23/10/2017 3:00 PM
-------------------------	-----------------------	--------------------

Font:Italic

Page 31: [29] Formatted	Microsoft Office User	23/10/2017 3:35 PM
-------------------------	-----------------------	--------------------

Font:Italic

Page 31: [29] Formatted	Microsoft Office User	23/10/2017 3:35 PM
-------------------------	-----------------------	--------------------

Font:Italic

Page 31: [30] Formatted	Microsoft Office User	23/10/2017 3:32 PM
-------------------------	-----------------------	--------------------

Font:Italic

Page 31: [31] Formatted	Microsoft Office User	23/10/2017 3:29 PM
-------------------------	-----------------------	--------------------

Font:Italic

Page 31: [32] Formatted	Microsoft Office User	23/10/2017 3:09 PM
-------------------------	-----------------------	--------------------

Font:Italic

Page 31: [33] Formatted	Microsoft Office User	23/10/2017 3:03 PM
-------------------------	-----------------------	--------------------

Font:Not Italic

Page 31: [34] Formatted	Microsoft Office User	23/10/2017 3:00 PM
-------------------------	-----------------------	--------------------

Font:Italic

Page 31: [35] Formatted	Microsoft Office User	23/10/2017 3:35 PM
-------------------------	-----------------------	--------------------

Font:Italic

Page 31: [35] Formatted	Microsoft Office User	23/10/2017 3:35 PM
-------------------------	-----------------------	--------------------

Font:Italic

Page 31: [36] Formatted	Microsoft Office User	23/10/2017 3:32 PM
-------------------------	-----------------------	--------------------

Font:Italic

Page 31: [37] Formatted	Microsoft Office User	23/10/2017 3:28 PM
-------------------------	-----------------------	--------------------

Font:Italic

Page 31: [38] Formatted	Microsoft Office User	23/10/2017 3:08 PM
-------------------------	-----------------------	--------------------

Font:Not Italic

Page 31: [38] Formatted	Microsoft Office User	23/10/2017 3:08 PM
-------------------------	-----------------------	--------------------

Font:Not Italic

Page 31: [39] Formatted	Microsoft Office User	23/10/2017 3:02 PM
-------------------------	-----------------------	--------------------

Font:Not Italic

Page 31: [39] Formatted	Microsoft Office User	23/10/2017 3:02 PM
-------------------------	-----------------------	--------------------

Font:Not Italic

Page 31: [40] Formatted	Microsoft Office User	27/02/2018 2:58 PM
Font:Italic		
Page 31: [41] Formatted	Microsoft Office User	23/10/2017 2:56 PM
Font:Not Italic		
Page 31: [42] Formatted	Microsoft Office User	23/10/2017 2:57 PM
Font:Italic		
Page 31: [43] Formatted	Microsoft Office User	23/10/2017 2:57 PM
Font:Italic		
Page 31: [44] Formatted	Microsoft Office User	27/02/2018 2:58 PM
Font:Not Italic		
Page 31: [44] Formatted	Microsoft Office User	27/02/2018 2:58 PM
Font:Not Italic		
Page 31: [45] Formatted	Microsoft Office User	23/10/2017 2:58 PM
Font:Italic		
Page 31: [46] Formatted	Microsoft Office User	23/10/2017 2:56 PM
Font:Not Italic		
Page 31: [46] Formatted	Microsoft Office User	23/10/2017 2:56 PM
Font:Not Italic		
Page 31: [47] Formatted	Microsoft Office User	23/10/2017 2:58 PM
Font:Italic		
Page 31: [48] Formatted	Microsoft Office User	23/10/2017 2:56 PM
Font:Not Italic		
Page 31: [49] Formatted	Microsoft Office User	23/10/2017 2:56 PM
Font:Not Italic		
Page 31: [50] Formatted	Microsoft Office User	23/10/2017 2:56 PM
Font:Not Italic		
Page 31: [51] Formatted	Microsoft Office User	23/10/2017 2:56 PM
Font:Not Italic		
Page 31: [51] Formatted	Microsoft Office User	23/10/2017 2:56 PM
Font:Not Italic		
Page 31: [52] Formatted	Microsoft Office User	23/10/2017 2:56 PM
Font:Not Italic		
Page 31: [52] Formatted	Microsoft Office User	23/10/2017 2:56 PM
Font:Not Italic		
Page 34: [53] Formatted	Microsoft Office User	05/03/2018 3:47 PM
Not Highlight		
Page 34: [53] Formatted	Microsoft Office User	05/03/2018 3:47 PM

Not Highlight

Page 34: [53] Formatted	Microsoft Office User	05/03/2018 3:47 PM
-------------------------	-----------------------	--------------------

Not Highlight

Page 34: [54] Deleted	Microsoft Office User	04/01/2018 4:26 PM
-----------------------	-----------------------	--------------------

Monthly statistics of modeled aerosol heights

Page 34: [54] Deleted	Microsoft Office User	04/01/2018 4:26 PM
-----------------------	-----------------------	--------------------

Monthly statistics of modeled aerosol heights

Page 34: [54] Deleted	Microsoft Office User	04/01/2018 4:26 PM
-----------------------	-----------------------	--------------------

Monthly statistics of modeled aerosol heights

Page 34: [54] Deleted	Microsoft Office User	04/01/2018 4:26 PM
-----------------------	-----------------------	--------------------

Monthly statistics of modeled aerosol heights

Page 34: [54] Deleted	Microsoft Office User	04/01/2018 4:26 PM
-----------------------	-----------------------	--------------------

Monthly statistics of modeled aerosol heights

Page 34: [54] Deleted	Microsoft Office User	04/01/2018 4:26 PM
-----------------------	-----------------------	--------------------

Monthly statistics of modeled aerosol heights

Page 34: [55] Formatted	Microsoft Office User	08/01/2018 1:01 PM
-------------------------	-----------------------	--------------------

Font:Not Bold

Page 34: [55] Formatted	Microsoft Office User	08/01/2018 1:01 PM
-------------------------	-----------------------	--------------------

Font:Not Bold

Page 34: [55] Formatted	Microsoft Office User	08/01/2018 1:01 PM
-------------------------	-----------------------	--------------------

Font:Not Bold

Page 34: [56] Formatted	Microsoft Office User	08/01/2018 1:03 PM
-------------------------	-----------------------	--------------------

Font:Italic

Page 34: [57] Formatted	Microsoft Office User	08/01/2018 1:05 PM
-------------------------	-----------------------	--------------------

Font:Italic

Page 34: [58] Formatted	Microsoft Office User	08/01/2018 1:06 PM
-------------------------	-----------------------	--------------------

Font:Italic

Page 34: [59] Formatted	Microsoft Office User	08/01/2018 1:07 PM
-------------------------	-----------------------	--------------------

Font:Italic

Page 34: [60] Formatted	Microsoft Office User	08/01/2018 1:08 PM
-------------------------	-----------------------	--------------------

Font:Italic

Page 34: [61] Formatted	Microsoft Office User	08/01/2018 1:01 PM
-------------------------	-----------------------	--------------------

Font:Italic

Page 34: [62] Formatted	Microsoft Office User	08/01/2018 1:05 PM
-------------------------	-----------------------	--------------------

Font:Italic

Page 34: [63] Formatted	Microsoft Office User	08/01/2018 1:05 PM
-------------------------	-----------------------	--------------------

Font:Italic

Page 34: [64] Formatted	Microsoft Office User	08/01/2018 1:06 PM
-------------------------	-----------------------	--------------------

Font:Italic

Page 34: [65] Formatted	Microsoft Office User	08/01/2018 1:07 PM
-------------------------	-----------------------	--------------------

Font:Italic

Page 34: [66] Formatted	Microsoft Office User	08/01/2018 1:08 PM
-------------------------	-----------------------	--------------------

Font:Italic

Page 34: [67] Formatted	Microsoft Office User	08/01/2018 1:01 PM
-------------------------	-----------------------	--------------------

Font:Italic

Page 34: [68] Formatted	Microsoft Office User	08/01/2018 1:05 PM
-------------------------	-----------------------	--------------------

Font:Italic

Page 34: [69] Formatted	Microsoft Office User	08/01/2018 1:05 PM
-------------------------	-----------------------	--------------------

Font:Italic

Page 34: [70] Formatted	Microsoft Office User	08/01/2018 1:06 PM
-------------------------	-----------------------	--------------------

Font:Italic

Page 34: [71] Formatted	Microsoft Office User	08/01/2018 1:07 PM
-------------------------	-----------------------	--------------------

Font:Italic

Page 34: [72] Formatted	Microsoft Office User	08/01/2018 1:08 PM
-------------------------	-----------------------	--------------------

Font:Italic

Page 34: [73] Formatted	Microsoft Office User	08/01/2018 1:01 PM
-------------------------	-----------------------	--------------------

Font:Italic

Page 34: [74] Formatted	Microsoft Office User	08/01/2018 1:05 PM
-------------------------	-----------------------	--------------------

Font:Italic

Page 34: [75] Formatted	Microsoft Office User	08/01/2018 1:04 PM
-------------------------	-----------------------	--------------------

Font:Italic

Page 34: [76] Formatted	Microsoft Office User	08/01/2018 1:06 PM
-------------------------	-----------------------	--------------------

Font:Italic

Page 34: [77] Formatted	Microsoft Office User	08/01/2018 1:07 PM
-------------------------	-----------------------	--------------------

Font:Italic

Page 34: [78] Formatted	Microsoft Office User	08/01/2018 1:08 PM
-------------------------	-----------------------	--------------------

Font:Italic

Page 34: [79] Formatted	Microsoft Office User	08/01/2018 1:02 PM
-------------------------	-----------------------	--------------------

Font:Italic

Page 34: [80] Formatted	Microsoft Office User	08/01/2018 1:05 PM
-------------------------	-----------------------	--------------------

Font:Italic

Page 34: [81] Formatted	Microsoft Office User	08/01/2018 1:04 PM
-------------------------	-----------------------	--------------------

Font:Italic

Page 34: [82] Formatted	Microsoft Office User	08/01/2018 1:06 PM
-------------------------	-----------------------	--------------------

Font:Italic

Page 34: [83] Formatted	Microsoft Office User	08/01/2018 1:07 PM
Font:Italic		
Page 34: [84] Formatted	Microsoft Office User	08/01/2018 1:08 PM
Font:Italic		
Page 34: [85] Formatted	Microsoft Office User	08/01/2018 1:02 PM
Font:Italic		
Page 34: [86] Formatted	Microsoft Office User	08/01/2018 1:05 PM
Font:Italic		
Page 34: [87] Formatted	Microsoft Office User	08/01/2018 1:04 PM
Font:Italic		
Page 34: [88] Formatted	Microsoft Office User	08/01/2018 1:06 PM
Font:Italic		
Page 34: [89] Formatted	Microsoft Office User	08/01/2018 1:07 PM
Font:Italic		
Page 34: [90] Formatted	Microsoft Office User	08/01/2018 1:08 PM
Font:Italic		
Page 34: [91] Formatted	Microsoft Office User	08/01/2018 1:02 PM
Font:Italic		
Page 34: [92] Formatted	Microsoft Office User	08/01/2018 1:05 PM
Font:Italic		
Page 34: [93] Formatted	Microsoft Office User	08/01/2018 1:04 PM
Font:Italic		
Page 34: [94] Formatted	Microsoft Office User	08/01/2018 1:06 PM
Font:Italic		
Page 34: [95] Formatted	Microsoft Office User	08/01/2018 1:07 PM
Font:Italic		
Page 34: [96] Formatted	Microsoft Office User	08/01/2018 1:08 PM
Font:Italic		
Page 34: [97] Formatted	Microsoft Office User	08/01/2018 1:02 PM
Font:Italic		
Page 34: [98] Formatted	Microsoft Office User	08/01/2018 1:05 PM
Font:Italic		
Page 34: [99] Formatted	Microsoft Office User	08/01/2018 1:04 PM
Font:Italic		
Page 34: [100] Formatted	Microsoft Office User	08/01/2018 1:06 PM
Font:Italic		
Page 34: [101] Formatted	Microsoft Office User	08/01/2018 1:07 PM

Font:Italic

Page 34: [102] Formatted	Microsoft Office User	08/01/2018 1:08 PM
--------------------------	-----------------------	--------------------

Font:Italic

Page 34: [103] Formatted	Microsoft Office User	08/01/2018 1:02 PM
--------------------------	-----------------------	--------------------

Font:Italic

Page 34: [104] Formatted	Microsoft Office User	08/01/2018 1:05 PM
--------------------------	-----------------------	--------------------

Font:Italic

Page 34: [105] Formatted	Microsoft Office User	08/01/2018 1:04 PM
--------------------------	-----------------------	--------------------

Font:Italic

Page 34: [106] Formatted	Microsoft Office User	08/01/2018 1:06 PM
--------------------------	-----------------------	--------------------

Font:Italic

Page 34: [107] Formatted	Microsoft Office User	08/01/2018 1:07 PM
--------------------------	-----------------------	--------------------

Font:Italic

Page 34: [108] Formatted	Microsoft Office User	08/01/2018 1:08 PM
--------------------------	-----------------------	--------------------

Font:Italic

Page 34: [109] Formatted	Microsoft Office User	08/01/2018 1:05 PM
--------------------------	-----------------------	--------------------

Font:Italic

Page 34: [110] Formatted	Microsoft Office User	08/01/2018 1:05 PM
--------------------------	-----------------------	--------------------

Font:Italic

Page 34: [111] Formatted	Microsoft Office User	08/01/2018 1:04 PM
--------------------------	-----------------------	--------------------

Font:Italic

Page 34: [112] Formatted	Microsoft Office User	08/01/2018 1:06 PM
--------------------------	-----------------------	--------------------

Font:Italic

Page 34: [113] Formatted	Microsoft Office User	08/01/2018 1:07 PM
--------------------------	-----------------------	--------------------

Font:Italic

Page 34: [114] Formatted	Microsoft Office User	08/01/2018 1:08 PM
--------------------------	-----------------------	--------------------

Font:Italic

Page 34: [115] Formatted	Microsoft Office User	08/01/2018 1:05 PM
--------------------------	-----------------------	--------------------

Font:Italic

Page 34: [116] Formatted	Microsoft Office User	08/01/2018 1:05 PM
--------------------------	-----------------------	--------------------

Font:Italic

Page 34: [117] Formatted	Microsoft Office User	08/01/2018 1:04 PM
--------------------------	-----------------------	--------------------

Font:Italic

Page 34: [118] Formatted	Microsoft Office User	08/01/2018 1:06 PM
--------------------------	-----------------------	--------------------

Font:Italic

Page 34: [119] Formatted	Microsoft Office User	08/01/2018 1:07 PM
--------------------------	-----------------------	--------------------

Font:Italic

Font:Italic

Figure 3: Time series of daily averaged measured AOD over the fire-constrained regions of the Maritime Continent [blue], and the non fire-constrained regions of the Maritime Continent [red], as given in **Figure 1**. Circles are computed daily mean values, while dots are computed daily standard deviation bands.

